A study of the seismic response of the city of Benevento (Southern Italy) through a combined analysis of seismological and geological data

G. Di Giulio[1], L. Improta[1], G. Calderoni[2] and A. Rovelli[2]

[1] Istituto Nazionale di Geofisica e Vulcanologia, Via del Castel D'Aquino, Grottaminarda (Av), Italy
[2] Istituto Nazionale di Geofisica e Vulcanologia, Via di Vigna Murata 605, Rome, Italy

corresponding author: digiulio@ingv.it
TEL: ++39 0651860613 FAX: ++39 0651860507

Abstract

A previous analysis (Improta et al., 2005) of small magnitude earthquakes recorded at 12 sites within the city of Benevento has stressed the significant role played by near-surface geology in causing variability of the ground motion. In this paper, we extend the study of the seismic response from 12 sites to the entire urban area. Based on inferences from the comparison at the 12 sites between earthquake and ambient vibration results, we have collected ambient noise at about 100 sites within the city, intensifying measurements across the main shallow geological variations. We use borehole data to interpret ambient noise H/V spectral ratios in terms of near-surface geology comparing H/V curves to theoretical transfer functions of 1D models along five well-constrained profiles.

On the basis of geological, geotechnical, and seismic data, we identify three main typologies of seismic response in the city. Each type of response is associated to zones sharing common soil conditions and similar soil classes according to building codes for seismic design. Moreover, we find that the spatial variation of the seismic response in the ancient town area is consistent with the damage pattern produced by a very destructive, well-documented historical earthquake that struck the city in 1688, causing MCS intensity of IX-X in Benevento.

Finally, we use ground motions recorded during the experiment by Improta et al. (2005) to generate synthetic seismograms of moderate to strong (Mw 5.7, Molise 2002 and Ms 6.9, 1980 Irpinia) earthquakes. We calibrate the random summation technique by Ordaz et al. (1995) using recordings of these earthquakes available in Benevento. After a satisfactory fit between observed and synthetic seismograms, we compute response spectra at different sites and speculate on effects of the geology class at large level of shaking, including soil nonlinearity. We find that large discrepancies from design spectra prescribed by seismic codes can occur for a wide sector of Benevento, especially for periods < 0.5 sec.

Keywords: *site effects, ambient noise, Empirical Green's Functions, response spectra, Benevento*

1. Introduction

The city of Benevento was the capital of the Sannio region (southern Italy). The ancient population of Samnites founded the city along the confluence of two rivers (Sabato and Calore rivers). After the third Samnite war (298-290 B.C.) Benevento was conquered by Romans becoming one of the most important

43 towns in southern Italy. In the Middle Ages the city was ruled by Lombards, by Byzantines (XI^{th} century)
44 and then by Popes.
45 Nowadays Benevento preserves an important historical heritage witnessing its long past. Significant
46 monuments within the city are the Trajan Arch (114 A.D.) built by the roman Emperor Trajan to celebrate
47 the win against Dacia, the Roman theatre and amphitheatre (I-II sec A.D.) and the church of Santa Sofia (762
48 A.D.). Benevento, with over 60.000 inhabitants at the present time, is a typical example of historical Italian
49 city showing a typology of buildings spanning from ancient to modern age. The precious monumental
50 heritage preserved in the old town is indeed surrounded by modern and densely populated areas.
51 The Sannio region is one of the Italian areas with highest potential for a future strong earthquake. This
52 region is surrounded by large seismogenetic structures such as Matese and Irpinia located about 20 km to the
53 north and 25 km to the south, respectively. These structures were responsible for five destructive earthquakes
54 that struck the town between 1456 and 1805, with magnitude ranging from 6.4 to 7.0 (Boschi et al., 2000).
55 Since 1805, the Sannio region experienced only one moderate event in 1962 (M_L 6.1; Westaway, 1987),
56 while the present-day seismicity is low and characterized by rare low-magnitude ($M<3$) swarms (Chiarabba
57 and Amato, 1997; Bisio et al., 2004). The long quiescence following the 1805 event makes Benevento to be
58 highly exposed to seismic hazard. In addition, local amplifications of the ground-shaking level are expected
59 in the urban area due to strong lithological changes and widespread soft soil conditions. Lithological
60 heterogeneities are indeed responsible for rapid variation of the shallow S-wave velocities (from 200 to 1700
61 m/s). Local site effects are also suggested by anomalies in the damage distribution (Castenetto and Romeo,
62 1992) during the strongest event experienced by the city in the 1688. Its local intensity was estimated to be
63 as large as X of the Mercalli-Cancani-Sieberg (MCS) scale.
64 For the aforementioned reasons, Benevento has been the subject of important projects for earthquake
65 risk mitigation (Mayer-Rosa, 1989 and 1991; Marcellini et al., 1991; Marcellini et al., 1995a; Traiano
66 project, 2002). The great deal of borehole data collected in the framework of these projects has been used to
67 define the shallow geologic structure and the geotechnical classifications, both however suffering of the
68 extreme subsoil complexity (Pescatore et al., 1996; Improta, 1998). Site effects in the city were investigated
69 by several authors based on the analysis of active seismic data (Iannaccone et al., 1995), 1D/2D numerical
70 modelling (Fäh and Suhadolc, 1994; Marcellini et al., 1995 b; Marrara and Suhadolc, 1998) and noise
71 measurements (Duval, 1994; Maresca et al., 2003).
72 Recently, Improta et al. (2005) installed temporary seismological stations in the city and analyzed local
73 ground motion applying standard spectral techniques. They used seismic noise and weak-earthquake
74 recordings ($2.1 \leq M \leq 5.5$; Fig. 1) collected from July 2000 until March 2004. These data were recorded at
75 twelve stations representative of the main soil categories present in the city (Fig. 2). The number of
76 earthquake data with a good signal-to-noise ratio ranges from 33 to 157 depending on the station. Seismic
77 data available at these sites were analyzed using classical site-reference (HHSR) (Borcherdt, 1970; Tucker
78 and King, 1984) and not-reference spectral techniques (HVNSR and HVSR) (Nakamura, 1989; Lermo and
79 Chavez-Garzia, 1994; Field and Jacob, 1995).
80 The present article is aimed at extending the analysis on local effects from few discrete sites to a large

sector of the urban area. Microtremor surveys are performed and results are interpreted taking into account geological/geotechnical constraints. The distribution of noise measurements was chosen to give spatial continuity to the information obtained at the twelve sparse sites. Seismic and geological data allow to identify three main typologies of local response and define the spatial areas of the city to be associated with each typology. The collection of weak earthquakes in seismogenic zones surrounding Benevento allowed the application of the Empirical Green's Function method to derive response spectra of moderate and strong magnitude (M 5.7 and 6.9) earthquakes at several sites. In this approach, the computed spectral ordinates include the effects of near-surface properties and are compared with values prescribed by seismic codes.

2. Geological Structure and Geotechnical classification

Results from crustal geophysical exploration indicate that the main upper structure in the Benevento area is a NW-trending syncline deforming a tectonic melange consisting of Miocene shales with sandstones and marly limestones (Fig. 3, bottom panel). This syncline is filled by Middle Pliocene conglomerates, sandstones and clays belonging to a typical regressive cycle. The city of Benevento spreads on the north-eastern margin of the syncline, where Quaternary continental deposits reach their maximum thickness (about 100 m) and cover both Miocene and Pliocene terrains (Fig. 3). Shallow geology in the urban area is extremely complex. Pescatore et al. (2005) recognizes a main ancient alluvial complex covering the pre-Quaternary substratum. This complex dates to Late Pliocene-Early Pleistocene times and consists of three facies: stiff cemented conglomerates (facies A), very dense gravels and sands (facies B) and palustrine fine soils (facies C) (Table 1). The geological evolution has been dominated since Early Pleistocene times by intense flooding-depositional and erosion alluvial cycles. The Calore and Sabato rivers, which encircle the ancient town (Figs. 2 and 3), are indeed responsible for several alluvial and palustrine Quaternary sequences, which are difficult to distinguish because of the variability of both grain size and cementation degree within the same sequence.

We use a subsoil model of Benevento which is based on borehole data collected and interpreted during previous studies (Marcellini et al., 1995a; Pescatore et al., 1996; Improta, 1998). About 250 boreholes drilled for civil engineering purposes provide information on the structure down to about 30-50 m depth (Fig. 3). The data set also includes boreholes specifically drilled for earthquakes hazard research projects, which allow an accurate lithostratigraphic characterization (Pescatore et al., 2005) (Fig. 3). In particular, seven 50 to 100 m deep drillings (Fig. 3) improve our knowledge on the hard-rock basement formations and shallow soil conditions with respect to previous studies.

The velocities for the main geological units of Benevento (Table 1) are mainly defined by means of cross-hole and down-holes surveys (Fig. 3). Only seismic refraction investigations are available for the Middle Pliocene sandstones/conglomerates and for the Miocene mélange, which exhibit P-wave velocity around 2600 m/s (Improta, 1998). We assign to these terrains a reference S-wave velocity of 1300 m/s setting the Vp/Vs ratio to 2 as inferred from local earthquake tomography in the Sannio area (Bisio et al., 2004). One cross-hole and 28 down-holes define the velocities for the near-surface geology (Table 1). The cross-hole from 100-m-deep boreholes located in the southern part of the Benevento hill (Lanzo, 1996)

provides accurate S-wave velocities (Vs) for the Middle Pliocene clays and for Late Pliocene-Pleistocene alluvial soils (Figs. 3 and 4). Three down-hole surveys (Fig. 4) from seismic hazard projects yield valuable information on the weathered Middle Pliocene clays, recent alluvia and superficial infillings (D'Onofrio et al., 2005). This information is complemented by results of 25 proprietary down-hole surveys from civil engineering companies. All in-situ measurements performed in sparse sites of the city provide consistent shear wave velocities within the same geological formations, indicating the reliability of Vs estimates (Fig. 4). A reliable soil column, complemented by a shear velocity profile inferred from the soil classification (Table 1), can be constructed down to 30-50 m depth in most of the recording sites. Therefore a site classification is possible in terms of shear-velocity for the uppermost 30 m (V_{S30}) according to the Eurocode 8 (EC8) prescription (CEN, 2003; ETC12, 2006) (Table 2).

The geological map of Figure 2 gives special emphasis to the near-surface soft layers (filling, colluvial soils, debris, recent alluvia) since they strongly contribute to worsen soil conditions in the flood plains and along the hill-side slopes. We complement this geological map with five geo-lithological cross-sections (Figs. 5a-e) and with a Vs section (Fig. 5f). The geological map, the two geological sections aa' and cc' and part of the section dd' have been already introduced in the previous work of Improta et al. (2005). Geological sections bb' and ee' and the Vs section are reconstructed in the aim of this study (Fig. 2). To construct the sections we used boreholes within less than 200 meters from the geological sections (Fig. 3). The distance can be larger for deep wells that constrain the pre-Quaternary substratum. In spite of the high density of boreholes that provide abundant constraints to the sections, some uncertainties remain in correspondence of lateral geological variations.

According to the geological structures, the city is divided into four sectors: the Capodimonte hill, the Sabato river plain, the Benevento hill and the Calore river plain (Figs. 2 and 3). For each sector, we indicate the site classification in terms of V_{S30} at the 12 stations used by Improta et al. (2005) (filled circles of Fig. 2; ARC1, MUS1, CAP2, CAL1, CAL2, CAL3, CAL4, CRE2, SAB1, SAB4, SAB5 and TEA1).

2.1 *Capodimonte hill*

Miocene shales are exposed in few outcrops east of the urban area in the Capodimonte hill, which corresponds to the north-eastern flank of the Pliocene syncline (Figs. 2 and 3). Borehole data indicate that the Miocene substratum is characterized by a superficial weathered, up to 15 m thick layer with a rapid improvement of the mechanical properties with depth (see the geological section of Fig. 5d). Among stations that provided earthquake recordings, CAP2 is the only one located on the Capodimonte Hill and is characterized by large Vs values (V_{s30} > 800 m/s according to Table 1; soil class A).

2.2 *Sabato river plain*

The Sabato river plain is a NNW-trending flat flooding plain about 1.5 km wide. The plain is bounded by the Gran Potenza ridge to the west and by the Benevento hill to the east (see Figs. 2 and 3, and the geological section of Fig. 5e). The Gran Potenza ridge is a quite regular NE-dipping monocline formed by Middle Pliocene terrains, sandstones and conglomerates in the lower part and stiff clays with silty levels in

the upper part. In the southernmost Sabato river plain, the Pliocene substratum consists of stiff clays with a near-surface weathered, several meters thick layer. In the northern part and along the eastern margin of the alluvial plain, the clayey Pliocene substratum rapidly deepens beneath deposits of the ancient alluvial complex (Late Pliocene-Early Pleistocene; Pescatore et al., 2005) (see the geological sections of Figs. 5a,c,e). This complex consists of a homogenous, some tens of meters thick layer of soft-to-consolidated fine soils referable to the palustrine facies C (Table 1). Boreholes located along the western slope of the Benevento hill document a lateral heteropic change from facies C to coarse alluvial deposits (facies A and B) that form the Benevento hill (see the geological sections of Figs. 5d,e). This transition is very rapid and causes strong Vs variations (Fig. 5f).

A shallow layer of Late Pleistocene-Holocene deposits (loose to dense coarse alluvia, filling, slope debris and soft colluvial soils) covers the Pliocene clays or the ancient alluvial complex (Fig. 5e). This superficial cover is characterized by poor mechanical properties (Vs as small as 200 m/s) and can exceed 15 meters of thickness along the boundaries of the plain.

The local soil conditions of sites TEA1, SAB1, SAB4 and SAB5 are characterized by V_{S30} ranging from 320 to 400 m/s, representative of soil classes B (SAB4) or C (TEA1, SAB1 and SAB5). Sites of class C share a low-velocity, about 10 m thick layer above fine palustrine soils (facies C).

2. 3 Benevento Hill

The Benevento hill is a NNW-trending ridge consisting of stiff cemented conglomerates with rare sandy lenses (facies A). The conglomerates outcrop along the crest of the ridge (see the geological sections of Figs. 5c,d,e). In the southern part of the Benevento hill, a 100-m-deep borehole well documents that the ancient alluvia overlie the Middle Pliocene stiff clays (Figs. 5d and 5e). Conversely, no drilling penetrates the pre-Pleistocene substratum in the old town and in the Cretarossa area. However, the thick formation of the cemented conglomerates, with S-wave velocities ranging from 1000 to 1730 m/s (see Table 1), well represents the bedrock formation of the Benevento hill in spite of its Pleistocene age.

In the northwestern sector of the hill, finer soils composed of very dense gravels and silty sands (facies B) interfinger with the cemented conglomerates. The coarse alluvia reach a total thickness of 60-70 meters and overlay consolidated palustrine soils (facies C).

In the eastern sector of the Benevento hill (e.g. Cretarossa terrace), the cemented conglomerates are covered by a younger fluvio-lacustrine deposit dating to Lower-Middle Pleistocene (Fig. 2 and Figs. 5b, 5c, 5d, 5e). This deposit consists of soft to consolidated fine soils, with sandy and gravelly lenses, and shows a progressive thickening moving north-eastward from the ridge crest (up to a thickness of about 25 m). Thick and heterogeneous covers of near-surface soft soils, including also reworked pyroclastites and debris of old buildings, are widespread on the Benevento hill. Fillings are negligible along the crest of Benevento hill that corresponds to the uppermost old town, and attain 10 meters in the southern, western and eastern sectors of the old town (see the geological sections of Figs. 5a,b,c). However, sudden thickenings of the superficial filling can also occur in the uppermost old town in correspondence of natural or artificial depressions of the

conglomeratic bedrock. Slope debris (very soft fine soils or loose sandy gravels) and colluvial deposits (often including reworked pyroclastites) encircle the hill-side slopes.

Site ARC1 and MUS1 are located in the uppermost old town on nearly outcropping conglomeratic bedrock (soil class A). The former was chosen as reference site in the HHSR analysis by Improta et al. (2005). CRE2 is on the Cretarossa terrace (soil class E).

2.4 Calore river valley

The pre-Pleistocene substratum in the Calore river valley consists of Middle Pliocene marine sediments that are reached by a well at about 70 m a.s.l. (Figs. 5a and 5b). The substratum is covered by deposits of the ancient alluvial complex: fine soils of facies C in the lower part and coarse soils of facies A in the upper part. The cemented conglomerates referable to facies A represent the seismic bedrock in the Calore river plain (Fig. 2 and the geological sections of Figs. 5a,b).

Sites CAL1, CAL2, CAL3, CAL4 (Fig. 2) in the Calore valley, similarly to CRE2, correspond predominantly to class E being characterized by a soft layer 5 to 20 m thick with low S-velocity overlaying stiff cemented conglomerates.

3. The ambient noise survey

Fig. 2 plots the HHSRs, relative to the reference bedrock site ARC1, and the HVNSRs for the twelve stations that provided earthquake recordings. The comparison at the twelve stations between ambient noise and earthquake data analysis (Improta et al., 2005) suggests the potentiality and the limit of noise techniques for assessing site effects in Benevento. HVNSRs yield reliable information on the seismic response in areas where bedrock consists of stiff conglomerates (Benevento hill, Cretarossa Terrace and Calore river Plain). Flat HVNSRs (maximum amplification less than 2) are found indeed for sites ARC1, MUS1, and CAP2 which belong to the same soil class A (Fig. 2, see also the geological sections of Figs. 5b,c). Consistently, the HHSRs of MUS1 and CAP2 do not show significant amplification relative to ARC1.

For sites CRE2, CAL1, CAL2, CAL3 and CAL4 the shapes of HVNSR and HHSR are also in good agreement; the narrow high-frequency peaks (amplitude of about 5 at $f > 4$ Hz) are well explained by 1D resonance of a soft layer above hard-rock basement (Fig.2, see also the geological sections of Figs. 5a,b,d).

Conversely, the sites of the Sabato plain (TEA1, SAB1, SAB4, SAB5 in Fig. 2, see also the geological sections of Figs. 5a,c,d,e) show the largest discrepancies between HVNSR and HHSR; the noise ratios are almost flat whereas earthquake data indicate moderate local effects in a large frequency band (amplification up to 7 in the frequency band 1-10 Hz). However, weak bumps around 1-2 Hz are observed in the HVNSRs of sites SAB4 and TEA1. These subtle bumps at low frequency could be dubitatively considered representative of the fundamental resonance of the sites (we will discuss this feature later).

Encouraged by the indications at sparse sites obtained from the comparison between earthquake and ambient noise analysis, and being confident on the knowledge of the shallow geology, we performed systematic microtremors measurements. We investigated about 100 new sites aligned along 5 main profiles well constrained by boreholes (Figs. 2 and 3). These profiles are tied to the 12 sites and cross the main geological

transitions. We use the HVNSR technique to map the spatial distribution of the resonance frequencies that are then interpreted in terms of local geology. In detail, the microtremor surveys are aimed at achieving the following targets:

- to explore the sensitivity of HVNSRs to the nature of surface covers and of substratum (Pleistocene conglomerates and Middle Pliocene clays in the Benevento hill and in the Sabato river plain, respectively);
- for environments with conglomeratic bedrock, to discriminate between areas where the resonance of the shallow low-velocity layers causes high-frequency amplification (i.e. narrow peaks in HVNSRs), and areas where no significant amplification occurs because of bedrock outcrops (i.e. flat HVNSRs);
- to evaluate the resonance frequencies in the old town, where local effects depend on widespread filling characterized by rapid variations of both thickness and shear-velocities. Moreover, to find out whether inferences based on ambient noise, earthquake results and geological constraints are confirmed by the damage distribution of the 1688 destructive earthquake;
- finally, to combine seismic and geotechnical/geological data in order to identify the spatial boundaries between areas with a different seismic response.

The spacing between adjacent measurement sites varies from about 100 m up to values as large as 500 m; the former is adopted in the old town and along the hill-side slopes affected by strong lateral variations, the latter in the central part of the Sabato plain which is a rather simple layered structure. All recording sites were far as much possible from sources potentially affecting the quality of noise recordings (industry, railway stations, underground parking, etc. etc.). We use a homogenous set of 6 stations composed of MarsLite digitizers equipped with Lennartz 3D-5s velocimeters using a sampling rate of 125 Hz. A time series of at least half-hour has been recorded at each site. The HVNSR has been computed following the processing procedures developed within the SESAME project (Site Effects Using Ambient Excitations [SESAME, 2004]). For each noise record, the stationary portion of the signal was selected adopting an anti-trigger algorithm to remove strong transients inside time histories. This selection provided, at each site, a number of at least 10 time windows 40 sec long. The time windows were detrended and 5% cosine tapered. The Fourier amplitude spectra were computed and then smoothed following Konno and Omachi (1998), with the parameter b set to 40. The two horizontal components spectra were combined into quadratic mean before dividing by the vertical component spectrum. The final geometric mean of the HVNSR and standard deviation are obtained by averaging the H/V ratios from all windows. Details on the software are in the SESAME deliverable no. D09.03 (http://sesame-fp5.obs.ujf-grenoble.fr/SES_TechnicalDoc.htm). The fundamental resonance frequency and the associated amplitude were visually selected from the HVNSR curves. The field-experiment took two days characterized by calm meteorological conditions.

4. Results of ambient noise data

The spatial distribution of the fundamental resonances resulting from the overall dataset of HVNSRs depends on the nature of geologic substratum. Figure 6 reveals that two areas can be roughly defined on the basis of the fundamental resonance frequency at high- or low-frequency. The first area includes large sectors of the Calore river plain, the Benevento hill and the Cretarossa Terrace, where HVNSRs show an evident spectral peak occurring above 3-4 Hz. In these sectors, superficial soft deposits cover the stiff basement composed of Pleistocene cemented conglomerates. The second area includes the Gran Potenza ridge, the Sabato river plain and the western slope of the Benevento hill (Fig. 6). Here, many sites show a HVNSR with a weak broad bump (amplitude less than 3) in the low frequency range (0.6-3 Hz) and the stiff Middle Pliocene clay can be assumed as substratum.

In Figures 5a-e we show, for each geological section, the contouring of HVNSRs linearly interpolated at adjacent sites. Moreover, we compare HVNSRs with S-wave 1D theoretical transfer functions (Haskell, 1960) for those sites where accurate subsurface information allows constructing realistic soil columns (upper frame of Figs. 5a-e). This comparison is aimed at assessing the reliability of the resonance frequency inferred from HVNSRs (Bonnefoy-Claudet et al., 2006; Gueguen et al., 2007).

Section aa' crosses from north to south the Calore river plain, the westernmost part of the old town and the Sabato river plain (Figs. 2 and 5a). In the first two sectors, the noise spectral content shows maxima at high frequencies that shift from about 10 to 8 Hz proceeding southward according to a thickening of shallow soft layers. The largest amplitude (about a factor of 5) of HVNSR occurs at site BB21 where soft fillings up to 10 m thick directly overlie cemented conglomerates (Fig. 5a). Moving further into the Sabato river plain, the peaks in HVNSRs jump to 3-5 Hz (sites BB3 and CAL4) and vanish afterward.

Sections bb' and cc' cross the old town and the Cretarossa terrace from west to east (Fig. 2). As shown in figures 5b and 5c, the HVNSRs are very sensitive to the thickness variation of fillings in the old town. Fillings are responsible for sharp peaked spectral ratios in the westernmost old town (CAL1, BB21, BB06). Flat HVNSRs are instead observed on the crest of the hill where the bedrock is nearly outcropping (BB07, ARC1, MUS1, BB20). However, maxima in the HVNSRs can occur in few isolated sites of the uppermost old town where depressions of the bedrock are filled by very soft materials including ruins of ancient collapsed buildings (i.e. site BB10, Fig. 5c). Sites located on the fluvio-lacustrine sediments of the Cretarossa Terrace exhibit high-frequency amplifications (sites BB22, BB11, BB14, BB16, CRE2; Figs. 5b,c). The sudden change in the shape of the HVNSRs at the edge of the old town (e.g. compare BB11 and MUS1 in Fig. 5b) is strictly related to local soil condition and well matches the margin of the Cretarossa Terrace. A correlation between the frequency where the HVNSR peak occurs and the depth of the conglomeratic bedrock is evident (e.g. compare site BB14 with BB16, Fig. 5b). HVNSRs do not show significant amplification in the southern part of the old town spreading on the Sabato river plain (Fig. 5c).

Section dd' extends from the Capodimonte hill to the northern-eastern edge of the Sabato river plain (Figs. 2 and 5d). No amplification is observed where Miocene rocks are outcropping. Moving westward into the Cretarossa terrace, HVNSRs confirm high-frequency resonance as shown by profiles bb' and cc'. The resonances shift from 4 to 8 Hz is in good agreement with the rise of the bedrock (sites CC04, CC06, CC07, CC09; Fig. 5d) that crops out along the crest of the Benevento hill (site CC12).

Section ee' extends from the Gran Potenza Ridge to the slope of the Benevento hill across the Sabato river plain (Fig. 2). Noise spectral ratios of Fig. 5e present amplification only at four sites located at the boundaries of the Sabato river plain near the Gran Potenza Ridge (CC26, AA15) and on the hill slopes (CC18, CC19). Their HVNSRs show high-frequency maxima (4-7 Hz) superimposed on the low-frequency weak bump suggesting a complex layered structure with velocity contrasts at very different scales.

Figures 5a-e and the spatial distribution of the fundamental resonance frequency (Fig. 6), which is the most relevant parameter in estimates of site effects, suggest a strict correlation between the shapes of the HVNSR curves and the shear-wave velocity local structure. To better illustrate the dependence of HVNSRs on the impedance contrast, in Fig. 5f we present a Vs section for a profile extending from the Cretarossa terrace to the Sabato river plain. The Vs section, partly overlapping the geological section dd' (see Fig. 3), has been obtained by linear interpolation of the 1D Vs profile associated to each borehole based on the soil classification. The comparison between Vs section and corresponding HVNSR contouring (Fig. 5f and 5d, respectively) confirms that i) a strong impedance contrast at shallow depth is responsible for high-frequency noise resonances observed in Cretarossa terrace; ii) nearly outcropping stiff conglomerates are consistent with flat HVNSRs observed in the upper part of the Benevento hill, and, iii) more ambiguous HVNSR curves are observed where the impedance contrast is weak, as in the Sabato river plain. A further comment concerns the comparison between HVSNRs and 1D theoretical transfer functions (Haskell, 1960). The best match between HVNSRs and 1D model is found for sites with narrow peaks at high frequencies ($f > 4$ Hz), as expected for uniformly layered structures with an impedance contrast larger than 3 (Bard, 1999; Bonnefoy-Claudet, 2004). According to Table 1 and Fig. 5f, the presence of very soft surface soils over shallow cemented conglomerates (8-15 m deep) can produce a velocity contrast larger than 5. This kind of sites shows a resonance at the highest frequencies ($f \geq 7$ Hz) (sites AA4, BB21, BB6, BB10 in Figs. 5a,b,c consistently with results obtained at CAL1, CAL2 and CAL3 in Fig. 2). The spectral noise peak appears broader and at lower frequencies where consolidated fluvio-lacustrine or dense coarse deposits are interspersed between shallow soft soils and bedrock. This causes a lower velocity contrast in most sites of the Cretarossa Terrace (e.g. sites BB11, BB14, BB16, CC7, CC6, CC4 consistently with CRE2) (Figs. 5b,d) and in a few sites in the northernmost Sabato river plain (e.g. sites BB3, CAL4) (Fig. 5a).

Borehole data and 1D modeling indicate that the fundamental resonance frequency ($f < 3$ Hz, see Fig. 6) observed in the Sabato plain can be associated to a deep, weak velocity contrast (< 2) existing in the Pliocene synform between clays and deeper sandstone/conglomerates (Table 1). Therefore, weak spectral bumps around 1-2 Hz (i.e. sites BB2, AA11, CC28 and CC29, Figs. 5c,e; sites TEA1 and SAB4 of Fig. 2) are diagnostic of the Pliocene stiff clays that represent the substratum of the Sabato river plain. The higher frequency content observed at sites along the hill-side slopes (i.e. CC26, AA15, CC19, CC18, Fig. 5e) is related to soft colluvial soils and debris (Vs around 200 m/s), which cover the large-scale layered structure of the Sabato river plain (Fig. 5f).

In general, the comparison at the 12 sites (Fig. 2) among HVNSR, 1D modelling and HHSR, shows a similar level of amplitude at the fundamental resonance frequency, as discussed in Improta et al. (2005). In spite of this similarity, no clear agreement has been established in literature concerning the accuracy of the

level of HVNSR peak as site amplification factor. The most recent explanations link the amplitude of HVNSR peak to the effects of converted waves (Parolai and Richwalski, 2004) and to the presence of Love waves within the noise wavefield (Bonnefoy-Claudet et al., 2007). From a quantitative point of view, a more reliable estimate of the site amplification factor is obtained through the S-wave transfer function computed on earthquake data, this technique having a stronger theoretical basis than HVNSR (nevertheless the selection of an appropriate reference site is crucial). Within these limitations, the amplitudes inferred from ambient noise give indication on the reliability of the resonance frequency but cannot be considered as a direct estimate of the amplification factor of sites (Sesame project, 2004).

5. Simulations of ground motion in Benevento using Empirical Green's Functions

The waveforms of small magnitude earthquakes located in seismogenic zones around Benevento (Fig. 1) and recorded at twelve sparse sites of the city (Improta et al., 2005) are now used as a catalogue of Empirical Green's Functions (EGF) representative of seismogenic sources of interest for the city. The technique consists in generating synthetic seismograms of larger earthquakes in far-field approximation using co-located low magnitude earthquakes (Hartzell, 1978; Joyner and Boore, 1986; Ordaz et al., 1995; Calderoni et al., 2005). The basic assumption is that the small event represents the Green's function for all points of the rupture area of the large earthquake. Following the Wennerberg (1990) approach, we assume a probability density function of the time delays over the rupture duration T of the target event. If the source spectra obey the omega-squared spectral model (Aki, 1967), the spectrum of the target earthquake [Targ] can be written as a random summation of the spectrum of the small event [subev]

$$\mathrm{Targ}(\omega) = w \cdot \mathrm{subev}(\omega) \sum_{j=1}^{N} e^{-i\omega t_j} \qquad (1)$$

where t_j is the shift time distributed in a random way within the rupture duration T, w and N are the scale factor and the number of stack, respectively. Their expressions are:

$$w = \left(\frac{M_{0,T\,\mathrm{arg}}}{M_{o,subev}} \right)^{-1/3} \left(\frac{\Delta\sigma_{T\,\mathrm{arg}}}{\Delta\sigma_{subev}} \right)^{4/3}$$

$$N = \left(\frac{M_{0,T\,\mathrm{arg}}}{M_{o,subev}} \right)^{4/3} \left(\frac{\Delta\sigma_{T\,\mathrm{arg}}}{\Delta\sigma_{subev}} \right)^{4/3} \qquad (2)$$

where $\Delta\sigma$ and M_0 are the Brune stress drop (Brune, 1970) in bar and the seismic moment in dyne·cm, respectively. They are related to the corner frequency of the event (f_c):

$$f_c = 4.9 \cdot 10^6 \beta \left(\frac{\Delta\sigma}{M_0} \right)^{1/3} \qquad (3)$$

where β is the S-wave velocity (3.5 km/s). The duration T is assessed through $(f_c)^{-1}$.

Under the assumptions of the method, this approach can be used to derive synthetics for a potential rupture in a seismogenic area starting from recordings of co-located small earthquakes. The method cannot be applied to close sub-events (source distance R must be significantly larger than the fault length L) because the omega-squared spectrum is a far-field model. We restrict the sub-event selection to low-magnitude events falling within the mesoseismal area of two recent moderate-to-large magnitude earthquakes: the Mw 5.7, 2002 Molise (Valensise et al., 2004) and the Ms 6.9, 1980 Irpinia earthquakes (Westaway and Jackson, 1987; Bernard and Zollo, 1989). These two cases are particularly suited because of the occurrence of two favourable conditions: i) distance from the faults was large enough to minimize the near-field terms, and ii) the level of excitation in Benevento was low minimizing the role of nonlinearity that might become significant at those magnitudes. For the two earthquakes, the availability of main-shock seismograms in Benevento allowed us to validate the technique of ground motion prediction for moderate-to-large magnitude earthquakes using weak events. After computing synthetics of the two target events through (1), we compare the acceleration response spectra on different geological formations with the shape of design spectra prescribed by seismic codes.

5.1 *Mw 5.7, 2002 Molise earthquake*

On October-November 2002 a seismic sequence, about 60 km north of Benevento, struck the southern part of Molise (Fig. 1). The two main shocks of October 31 and November 1, 2002 were characterized by a pure-lateral strike slip over a east-west striking fault and attained Mw 5.7 (Valensise et al., 2004). Macroseismic MCS intensity of Benevento was IV. The twelve stations installed in Benevento recorded the entire sequence. Unfortunately, the seismograms of the two largest shocks were clipped at ±0.25 cm/s due to the digital saturation. Despite the limitation of clipping, these data can be suitably used for many research applications because: i) saturation did not affect the first 10-12 sec of the recordings, where is concentrated the largest part of the high-frequency content of the mainshocks; ii) at the rock reference station (ARC1), the amplitude underestimation due to saturation was of the order of 5% (a detailed discussion can be found in Calderoni et al., 2007). Therefore, the spectral estimate on the entire record of ARC1 was not significantly affected by clipping. However, we computed the conventional spectral ratios (with ARC1 as reference site) for the two Molise mainshocks using the unclipped portion of the seismograms. These spectral ratios overlap the ±1 s.d. interval estimated through weak motions (Improta et al., 2005). This confirms that, as expected, nonlinear effects did not occur at such low ground shaking level (less than 10 gals).

Thus, the random summation method is used to construct synthetic ground motions at stations where the recordings were clipped. Synthetic seismograms for the Mw 5.7 shock have been generated starting from two of the largest aftershocks (Mw 3.7 and 3) of the Molise sequence recorded in Benevento. We have applied the technique of Ordaz et al. (1995), constraining low- (through seismic moments) and high-frequency (through stress drop) amplitudes. The analyzed frequency band was 0.5-10 Hz. According to the scaling law found by Calderoni et al. (2007) we use a value of 8 bars for the mainshocks and 4 and 2 bars for two subevents. We first checked the suitability of the method by comparing true (clipped) and synthetic

ground motions for the stations in Benevento. The same clipping (0.25 cm/s) of real data has been applied to synthetics. Figure 7 shows a good consistency in amplitudes and duration between clipped synthetics and real seismograms for stations in Benevento that recorded the aftershocks. The synthetic seismogram that best reproduced the duration of clipping and the amplitudes of the real seismograms was selected as representative of ground motion of the Mw 5.7 earthquake in Benevento. This allowed us to use the best (unclipped) synthetics of the Mw 5.7 earthquake and to compute the corresponding elastic spectra. Figure 8 shows the 5% damped acceleration response spectra of the synthetics of the Mw 5.7 earthquakes for the two horizontal components. These spectra are compared with the Sabetta and Pugliese (1996) expectations for stiff and shallow alluvium (dashed-dotted and dashed curves in Fig. 8, respectively) computed at the same magnitude and source distance (Mw 5.7 and R 60 km). The design response spectra prescribed by the National code (''Norme Tecniche per le Costruzioni'' of September 23, 2005), for the different soil classes (Table 2), are also included. The Italian building code prescribes i) to anchor the shape of the design spectra to the maximum horizontal ground acceleration on bedrock (PGA), and, ii) to adopt a different PGA for class1 and class2 buildings (probability of exceedance of 10% and less than 5% in 50 years, respectively). We first anchored the shape of design response spectra at T=0 sec to the PGA predicted at stiff-site by the Sabetta and Pugliese (1996) regression for that magnitude and source distance. Figure 8 (left panel) shows that amplitudes of the two Mw 5.7 Molise shocks are significantly smaller than both the statistical expectations of Sabetta and Pugliese (1996) and the National code prescriptions. This effect is due to the low energy release of 2002 Molise events which are about 10 times smaller in stress drop than moderate-magnitude normal-faulting earthquakes in the Apennines, as discussed in Calderoni et al. (2007).

To emphasize relative variations of response spectra between stations, we have anchored the design spectra at T=0 sec to the PGA value (about 4 gals) estimated for the rock reference site (ARC1). Figure 8 (right panel) indicates that the shapes of response spectra vary consistently with the local geology. The soft sites TEA1, CAL4 and SAB5 show, at short periods (T < 1 sec), larger spectral ordinates than the rock site ARC1, thus exceeding the design response spectrum of soil class B and C (representative of soft sites).

5.2 *Ms 6.9, 1980 Irpinia earthquake*

A second check on the reliability of the EGF approach deals with the Ms 6.9, 1980 Irpinia earthquake. It was recorded in Benevento by an SMA-1 analog accelerograph located at the southern limits of the Benevento hill (see cross symbol in Figs. 2, 3 and Fig. 4). The accelerograph was installed on very dense gravely soils and consolidated clays, which belong to the facies B of the ancient alluvia formation. The cross-hole of Fig. 4 (Lanzo, 1996) documents a V_{S30} > 800 m/s (soil class A according to EC8). The available recording in Benevento shows a PGA of about 50 gal for this event characterized by a local MCS intensity of VI (Boschi et al., 2000).

Two co-located small events of magnitude around 3 were recorded by our stations. Their epicentres are located within the seismogenetic area of the 1980 event (Fig. 1). These two events were used to generate synthetics in the frequency band 0.5 < f < 10 Hz, where signal-to-noise ratio of the weak motions resulted to be larger than 3. The weak motion of co-located events, recorded in several sites of the city, allows us to

456 derive the Ms 6.9 synthetics for the different soil categories. We use a stress drop of 100 bars (Cocco and
457 Rovelli, 1989) for the mainshock and 30 bars for the subevents. Figure 9 (upper frame) compares the
458 response spectra of the accelerogram recorded in Benevento with those simulated using the weak motions of
459 ARC1 and MUS1, which share the soil class A being located on stiff cemented conglomerates. The
460 agreement of response spectra between Ms 6.9 recorded and Ms 6.9 simulated is satisfactory, with a
461 maximum discrepancy of about 30% limited to a very narrow interval of periods (around 0.2 sec). Figure 9
462 (bottom frame) also shows the acceleration response spectra for the Ms 6.9 synthetic seismograms at the
463 stations in Benevento that recorded the M 3 earthquakes. The response spectra simulated using EGFs are
464 overimposed to the design spectra of the national ordinance anchored to the PGA predicted by Sabetta and
465 Pugliese (1996) for rock site (Fig. 9). Adopting this PGA anchoring, the spectral ordinates of sites in the
466 Sabato river valley largely exceed the design spectra of class B and C especially for periods less than 1 sec.
467 The response spectra of the Ms 6.9 synthetics at sites ARC1 and MUS1 agree, on the average, with the
468 shapes of response spectra prescribed by the National code for soil class A (Fig. 9). A good fit is also
469 observed for site CRE2 (soil class E), although the spectral ordinates at T=0.2 sec slightly exceeds the
470 plateau of design response spectra. The comparison between Fig. 9 and Fig. 8 (right panel) shows a general
471 agreement, in terms of local amplifications at the different sites, between results inferred from the synthetics
472 of the Molise and Irpinia earthquakes.
473 In order to assess the role of soil nonlinearity in modifying the spectral amplification, we consider
474 nonlinear models applied to the soil types of Benevento. We include variation of shear modulus and damping
475 ratio with shear strain following Marcellini et al. (1995a) and Lanzo (1996), who assigned mechanical
476 properties to the soil classes in Benevento through cyclic and dynamic laboratory tests and correlation with
477 index properties. The cyclic soil behaviour is described assuming a linear-equivalent approach according to
478 the Ramberg-Osgood-Masing model (Silvestri, 1991). We consider the soil nonlinearity for SAB5 since this
479 site shows the largest spectral ordinates (see Fig. 9). We assume that the Ms 6.9 seismograms recorded in the
480 Benevento hill can be adopted as bedrock-input-motion for site SAB5 located in the Sabato river plain.
481 Therefore we convolve the seismogram of the Ms 6.9 earthquake recorded at the stiff site with the soil
482 column of SAB5 (see Fig. 2) using an equivalent-linear approach (EERA code, Bardet et al. 2000). At each
483 type of soil of SAB5, a corresponding curve of shear modulus and damping ratio is assigned. Fig. 10 shows
484 the acceleration response spectra of the Ms 6.9 accelerogram recorded at the cross-hole stiff site in
485 Benevento for the two horizontal components. Fig. 10 also shows the response acceleration spectra of
486 synthetics computed through convolution of stiff site seismograms with the soil column of SAB5. The
487 convolution was performed both taking into account the soil nonlinearity and adopting a constant shear
488 modulus with no damping variation. As shown in Figure 10, we observe that the main effect of soil
489 nonlinearity is to decrease of about 15% the largest spectral ordinates at about 0.2 sec on the EW component.
490 The negligible amplitude depletion induced by soil nonlinearity at low periods is consistent with the
491 relatively low ground shaking level caused by a Ms 6.9 event at 50 km of distance (about 50 gal at rock
492 sites).
493

6. Inferences on site effects during the 1688 destructive earthquake

The results previously discussed emphasize a strong dependence of ground motions on local geology, in the range from ambient vibrations up to 50 gals. We now use seismic and geological information to investigate a possible role of site effects in increasing the damage during an earthquake with destructive effects in Benevento. The damage pattern of the 1688 Sannio earthquake (Me 6.7; Boschi et al., 2000), which is the most destructive one experienced by the city (local MCS intensity of X, Fig. 1), can shed light on this issue. Starting from detailed historical chronicles of this event, Castenetto and Romeo (1992) reconstructed the spatial distribution of the damage in the old town (Fig. 6 and Fig. 11). The most damaged zone, with more than 75% of buildings collapsed, was the south-western one extending towards the Sabato river plain (Fig. 11). Damage was lower (less than 50% of buildings collapsed) along the crest of the hill whereas intermediate damage (50-75 % of building collapsed) was reported for the north-western and eastern sectors, the latter corresponding to the Cretarossa Terrace.

Recordings of small magnitude earthquakes are available for four sites of the historical area (Fig. 11): TEA1 and CAL4 in the most damaged zone, ARC1 and MUS1 in the area that experienced the lowest level of damage, whereas no earthquake data are available in the zones of intermediate damage.

The lower level of ground motion observed at the hard-rock sites ARC1 and MUS1 for weak earthquakes is consistent with the lowest damage. The HHSRs at soft sites TEA1 and CAL4 (using ARC1 as reference site) document both broad-band and high-frequency effects in the mostly damaged zone. Similar site effects are also shown by HHSRs of sites CAL1, SAB1 and SAB4 (Figs. 2 and 11). Although these sites are outside the target area, they surround the zone that suffered the strongest damage toward the west and the south, respectively.

Ambient noise data are available at numerous sites in the old town (Fig. 11). In the lowest damage zone, the HVNSRs show a predominant flat shape. In intermediate damage zones, HVNSRs indicate a distinct 1D resonance. In the most damaged sector, HVNSRs identify fundamental resonance both at low- and high-frequency (broad spectral bumps and narrow peaks, respectively) (Fig. 11).

However, HHSR and HVNSR provide a relationship between site effects and damage that is only qualitative and cannot be applied, a priori, for destructive earthquakes because of possible nonlinear behaviour of soil. This aspect is now faced by means of a real record of the Ms 6.9, 1980 Irpinia earthquake. We use the strong motion accelerogram of the hard-rock station of Sturno located about 30 km south of Benevento (Fig. 11). Recordings show PGA of 0.25 and 0.36 g for the NS and EW horizontal components, respectively. We adopt the same procedure explained above for Fig. 10. The Sturno accelerograms are first assumed as input-bedrock-motion in Benevento and then are convolved with the non-linear response of the soil column of sites using an equivalent linear approach. After the convolution we compare the acceleration response spectra of sites in the historical area with the design spectra. According to the National decree (‘’Norme Tecniche per le Costruzioni’’ of September 23, 2005) that assigns the PGA value of 0.35 g to class 1 buildings in the whole area of Benevento, we anchor the design response spectra at T=0 sec to this value. The acceleration response spectra (Fig. 11) in the lowest damage zone of stiff sites (ARC1 and MUS1; i.e. soil class A) are below the design spectra, on the average. In the intermediate and most damaged sectors, the

spectral content is well above the design spectra especially for T < 0.5 sec. At periods between 0.5 and 1 sec, the response spectra of TEA1 show a spectral content larger than the other sites (Fig. 11).

To sum up, the lowest damage zone of the 1688 earthquake corresponds to the uppermost area of the old town where stiff conglomerates are nearly outcropping (soil class A) and consistently we found not significant site effects (see also Fig. 5f). In the intermediate damage zone, a spectral increase at high-frequencies with respect to the hilltop is related to the resonance of superficial filling and fluvio-lacustrine soft deposits. The response spectra, computed including the near-surface soil properties, document narrow high peaks (amplitude > 2 g) at periods < 0.5 sec. In the southern sector of the old town, which experienced the most severe damage, we found spectral magnification in the largest frequency band (1-10 Hz) (Fig. 11).

Furthermore, building vulnerability must be taken into account in relating damage to ground motion. During the 1688 earthquake, the vulnerability was likely rather uniform in the urbanized area but for potential future large earthquakes vulnerability could play an important role. The existing urban settlement is very heterogeneous showing typologies of construction that range from medieval to modern age. Recent and very densely populated areas spread in the Sabato river plain. Part of this plain was urbanized between the 1940s and 1960s, with popular buildings mostly of rectangular shape (3-5 stories) and composed of reinforced concrete of poor quality (Pecce et al., 2004). For this kind of structures, an estimate of damage scenario in the Sabato plain yields a large percent of collapses in case of a strong earthquake (Cosenza et al., 2005). Recent buildings were built with reinforced concrete in the zones of Cretarossa Terrace and Calore river valley, whereas old masonry and stone structures are common in the old town. The soil resonance often observed at f ≥ 4 Hz could be reasonably close to the resonance frequency of small structures at 3-5 stories widespread in Benevento.

Finally, we want to characterize quantitatively the different typologies of seismic response during significant earthquakes. We consider the integral of the acceleration response spectra within periods 0-2 seconds at sites where we have estimated numerically strong ground motions. An amplification factor (AF) at each site is assessed through the ratio

$$AF = \frac{\int_{T=0}^{2} S(T)dT}{\left(\int_{T=0}^{2} S(T)dT\right)_{STIFF\_SITE}} \qquad (4)$$

where S is the acceleration response spectrum computed using synthetics of the simulated cases (the Mw 5.7 Molise event, the Ms 6.9 Irpinia earthquake and the scenario using the Sturno recordings; see Figs. 8, 9 and 11, respectively). The results are shown in Table 3. As expected, the significant role of surface geology is confirmed in terms of response spectra with variations from AF close to 1 at stiff sites (soil class A) up to more than 2 at sites in the Sabato river valley.

7. Conclusions

We first mapped the spatial variations of the fundamental resonance frequency within the city by means of noise data analysis. Then, we focused on five profiles well-constrained by boreholes and crossing the

567 main geologic environments to explore the sensitivity of microtremors to the variations of near-surface
568 properties. We found a clear dependence of the noise spectral ratios on the shallow soil conditions and the
569 type of stiff-rock formation. These results, combined with the indication given by earthquake recordings at
570 twelve sites, legitimated us to define the spatial boundaries between zones that should undergo a different
571 seismic response. Seismic analysis and local geology consistently discriminate three main typologies of
572 seismic response during weak-to-moderate ground motion (Fig. 12): (I) relative low amplification (light grey
573 in Fig. 12), (II) 1D resonance with a sharp high-frequency ($f \geq 4$ Hz) peak (intermediate grey), and (III)
574 moderate amplification in a wide frequency band (1-10 Hz) (dark grey).
575 The three kinds of local response are representative of the soil classes within the city depending on V_{S30}
576 and velocity contrasts. Behaviour of type I characterizes areas where hard-rock formations (Pleistocene
577 cemented conglomerates or Miocene rocks) are nearly outcropping. This is the case of the uppermost old
578 town spreading along the crest of the Benevento hill where V_{S30} exceeds 800 m/s (soil class A) (Fig. 5f).
579 Spectral peaks of type II are observed in the northwestern and eastern sectors of the city consistently with a
580 strong velocity contrast at shallow depth (Fig. 5f). These sites belong predominantly to soil class E
581 widespread in the Calore river valley and in the Cretarossa Terrace.
582 A response of type III is typical of the Sabato river plain. It is likely controlled at low frequency ($f < 2$ Hz)
583 by the weak velocity contrast between the Pliocene stiff clays and the underlying sandstones/conglomerates.
584 The resonance of shallow soft soils contributes to amplify ground motion at higher frequencies. Local soil
585 conditions in the Sabato river plain are indicative of soil class B or C.
586 Interestingly, the spatial distribution of the seismic responses in the old town (Fig. 12) well correlates with
587 the damage pattern caused by the strongest historical earthquake experienced by Benevento (1688, local
588 MCS intensity of X).
589 Besides contributing to the microzonation of the city, the waveforms of weak earthquakes recorded in
590 Benevento were used to describe shaking features of moderate-to-large magnitude earthquakes using the
591 Empirical Green's Function (EGF) technique. Calibration tests adopting the random summation method by
592 Ordaz et al. (1995) were performed for the Irpinia 1980 (Ms 6.9) and Molise 2002 (Mw 5.7) earthquakes,
593 whose recordings are available in Benevento. We obtain a satisfactory fit between observed and synthetic
594 seismograms. This allows us to extend our discussion on local effects in terms of design response spectra
595 that are computed for the soil categories present in Benevento. The Irpinia and Molise synthetics consistently
596 show large amplifications at soft sites (Table 3). A difference is found in terms of absolute amplitudes of
597 acceleration response spectra. Using the anchoring PGA predicted by the attenuation law usually adopted in
598 Italy (Sabetta and Pugliese, 1996), the Irpinia earthquake results to exceed at low periods the design spectra
599 especially at sites of the Sabato river valley (Fig. 9). In contrast, the spectral ordinates of the low stress drop
600 Molise event are well below the design spectra (Fig. 8 left). In order to speculate on a larger level of shaking,
601 we assume the seismograms of a near-source rock-station (Sturno) of the Irpinia earthquake as input for
602 Benevento. The acceleration response spectra, computed including soil nonlinearity (Fig. 11), confirm that
603 the largest discrepancies with design spectra still occur for sites with seismic response of type II and III,
604 especially for periods < 0.5 sec. If we group the stations of Table 3 according to the three seismic response

typologies and compute the average amplification factor (<AF>) and the 1 standard deviation interval, we found that amplification increases from type I to type III, with a large average value (more than a factor of 2) that is found for the southern part of downtown Benevento and the Sabato river plain (Fig. 12). The values of <AF> for each typology with their statistical uncertainties are shown in the inset of Fig. 12. It is worthy of note that the one standard deviation intervals around the mean are well separated among the three kind of seismic responses.

The case study of Benevento shows that a combined analysis of geological and seismological data can be useful to investigate the seismic response and to discriminate the near-surface soil conditions. These indications are of clear interest, in urban areas, to the local authorities and to the civil engineering community dealing with strategies for seismic risk mitigation (taking in account the seismic codes). From a practical point of view, the collection of earthquake data at sites sampling different geological environments of an urban area is a difficult task, especially in regions with a low rate of seismicity. Hence seismic microzonation studies largely employ the single-station noise technique because of its low cost, low time-consuming and simplicity of use. As well-known in the literature, the HVNSR yields the best evidences of site effects in presence of strong velocity contrast caused by soft layer above a stiff basement. In this case, the HVNSRs show a clear resonance peak (response of type II in the present paper) which is, for 1D structures, closely related to the thickness and Vs of the soft soil. Recent studies (Panou et al., 2005; Cara et al., 2007) assess the spatial distribution of soft sediments in urban environments using a large number of noise measurements, finding a promising correlation between HVNSR results and damage pattern caused by past earthquakes of engineering importance. However, it is important to stress that the H/V noise method, in presence of complex geological conditions or weak velocity contrast (such the Sabato river plain), can lead to erroneous interpretation in evaluating the depth or the average shear-wave velocity of deposits. The reliability of noise measurements should be therefore validated by independent geological/geophysical/seismological approach when the 1-D model assumption is not fully verified.

Acknowledgements

This research was conducted with INGV internal research funds and the contribution of the MIUR Prosis Project. The seismic network in Benevento was financed by the GNDT Traiano Project. We are grateful to Fabrizio Cara, Angela Chesi, Giovanna Cultrera, Carlo De Santis, Rosalba Maresca and the students of the University of Sannio for their help during the noise measurements. Special thanks are due to the Associate Editor and to two reviewers for their constructive comments. We thank Maria Rosaria Senatore, Tullio Pescatore, Modestino Boscaino and Massimiliano Romito for useful discussion on the Benevento geology. We also thank Anna D'Onofrio who kindly provided down-hole data.

643 **Figure captions**

644

645 **Figure 1** - Epicentres of the small magnitude ($2.1 \leq M \leq 5.5$) earthquakes (open circles) recorded by 12
646 seismic stations in Benevento, used by Improta et al. (2005) to estimate the local response. The black
647 continuous and dashed lines correspond to isoseismals of large historical earthquakes that struck the city in
648 1688 (Io=XI of the MCS scale), 1702 (Io=X), 1732 (Io=X) and 1805 (Io=X). Focal mechanisms and
649 epicentres (white stars) of the 1980 Ms 6.9 Irpinia (1) and of the 2002 Mw 5.7 Molise earthquakes (2) are
650 also shown.

651

652 **Figure 2** - Geologic map of Benevento (redrawn from Improta et al., 2005). The geological units are
653 described in Table 1. The dashed black lines indicate the five geological sections (aa', bb', cc', dd', ee'). The
654 red line bounds the old town. The filled stars and circles show sites of the microtremor survey and location
655 of 12 seismic stations, respectively. For each of the 12 stations we draw the previous results by Improta et al.
656 (2005) plotting i) the HHSR (± 1 standard deviation around the mean value) using the site ARC1 as
657 reference for the earthquakes of Fig. 1, and, ii) the HV noise spectral ratio. We also plot the 1D theoretical
658 transfer function (dashed lines). We also indicate the soil class as defined by National decree (''Norme
659 Tecniche per le Costruzioni'' of September 23, 2005) (Table 2). For Type E soil, the average shear velocity
660 of the surface alluvium layer is indicated as Vs_{BED} .

661

662 **Figure 3** - (Upper panel) Position of the boreholes (modified after Improta et al., 2005) used in this study to
663 construct the five geological sections (black lines). Boreholes are grouped on the basis of the available
664 information: (1) only stratigraphy; (2) stratigraphy and Standard Penetration Test (SPT); (3) stratigraphy and
665 laboratory measurements; (4) stratigraphy, SPT and laboratory measurements; (5) Down-hole surveys; (6)
666 Cross-hole survey; (7) deep ($50 < z < 90$ m) exploration wells with detailed core analysis. The dashed line
667 bounds the old town. The dotted grey line indicates the Vs section of Fig. 5f.
668 (Lower panel) Schematic geologic section of the upper crust in the Benevento area based upon commercial
669 reflection profiles, refraction and gravity data modelling.

670

671 **Figure 4** – Comparison of Vs vertical profiles for down-hole and cross-hole surveys carried out in different
672 geological environments of Benevento. The inset map shows the location of boreholes. Down-holes DH1
673 and DH2 were performed for civil engineering investigations, DH3 in the framework of a seismic
674 hazard research project (Anna D'Onofrio, personal communication), cross-hole CH1 is redrawn
675 from Lanzo (1996). Note the consistency of Vs values within the same geological formations (as
676 described in Table 1).

677

678 **Figure 5a-e** - Geological cross-sections and coloured contouring of HVNSRs (mean). The geotechnical
679 classification is described in Table 1 and the sections traces are reported in Figures 2 and 3. The vertical
680 black lines in the geological sections indicate the positions and depth of boreholes. The 12 seismic stations

with earthquake data are shown as black filled triangles. Sites of microtremor measurements with an accurate subsurface characterization are indicated as grey circles. The H/V noise spectral ratios (± 1 standard deviation around the mean) of these sites are plotted in the upper frame. All sites are classified according to the EC8 code. For soft sites (soil classes B, C, E), the noise spectral ratios are compared with 1D S-wave theoretical transfer function (thick dashed lines) using the soil column on the left. Geological sections of Fig. 5a, 5c and 5d are modified after Improta et al. (2005).

Figure 5f – Shear-wave velocity section across the Sabato river plain and the Cretarossa terrace. The section trace is reported in Figure 3 as dotted grey line. The Vs section has been obtained by linear interpolation of 1D Vs profile associated to each borehole based on the soil classification. The arrows indicate the projections of the used boreholes.

Figure 6 - Fundamental resonance frequencies and associated amplifications estimated through H/V noise ratios (upper and lower panel, respectively). The size of triangles is proportional to the values of frequency (top) and amplification (bottom). Squares depict nearly flat H/V ratios (i.e, without clear peaks; amplitude values less than 2) or H/V ratios showing unclear low-frequency bumps. Grey symbols refer to the twelve sparse seismic stations. The traces of the geological sections are also shown. The latitude and longitude values are in Gauss-Boaga projection. The thin black lines, in the upper frequency map, bound the sectors that suffered a different level of damage during the 1688 earthquake (after Castenetto and Romeo, 1992).

Figure 7 - Real seismograms (at sites ARC1, TEA1, SAB5 and CAL4) of the October 31, 2002, Molise mainshock (upper waveforms) of the two horizontal components are compared with two synthetic seismograms modelled from weak motions through Eq. 1 (EGFs). We have applied an artificial clipping at the synthetics using the same saturation threshold of the real data: the consistency between real and synthetic seismograms guarantees the reliability of results.

Figure 8 - The thin black lines depict the 5% damped acceleration response spectra of the two horizontal components computed from synthetics of the Mw 5.7 Molise earthquakes for a source distance of R=60 km. (Left) The design acceleration spectra (as prescribed by National decree ‘’Norme Tecniche per le Costruzioni’’ of September 23, 2005 for class 1 building and for different soil classes) are plotted as thick grey curves and their shapes are anchored at T=0 sec to the PGA predicted by the Sabetta-Pugliese regression for stiff site. The Sabetta-Pugliese regressions for deep and shallow alluvium are plotted as dashed-dotted and dashed curves, respectively. Note the spectral deficit of the 2002 Molise earthquakes. (Right) The shapes of design spectra are anchored to the PGA of the reference rock site (ARC1).

Figure 9 – (Top) Acceleration response spectra of the Ms 6.9, 1980 Irpinia earthquake for a stiff-site accelerogram recorded in Benevento (black and grey continuous lines for NS and EW components, respectively) are compared with the response spectra computed from synthetics of MUS1 and ARC1 (dashed

lines). Synthetics were generated through EGFs of co-located weak-motion earthquakes. Note the significant consistency between real and synthetic data for stiff sites. (Bottom) The response spectra of synthetics for the 1980 Irpinia earthquake computed for both hard-rock and soft-soil sites are compared with the shape of design response spectra (National decree ‘’Norme Tecniche per le Costruzioni’’ of September 23, 2005); the latter are anchored to the PGA of the Sabetta-Pugliese regression for stiff-site. The grey areas confine the envelopes of response spectra computed on the two horizontal components of synthetics.

Figure 10 - Response spectra of the Ms 6.9, 1980 Irpinia earthquake computed from a stiff-site accelerogram recorded in Benevento (EW and NS components) are compared with response spectra after convolution with the soil profile of SAB5. The modelling was performed both with and without soil nonlinearity.

Figure 11 – (Top) Horizontal components of the Ms 6.9, 1980 Irpinia recorded at the station of Sturno. (Bottom) Map of the old town with the damage variations caused by the 1688 earthquake (modified from Castenetto and Romeo, 1992). The largest, intermediate and smallest damage zones are in heavy, intermediate and light grey, respectively. The dashed-thick black line shows the extension of the town during Roman times; the absence of grey shadowing indicates the sector where no damage information is available. Recording sites are classified according to the shape of the H/V noise ratios: sharp peaks at $f > 3$ Hz (filled triangles), weak low-frequency bumps (open triangles), nearly flat ratios (filled squares). HHSRs, HVNSRs and response spectra of the Sturno-convolved-seismograms (continuous and dashed lines for EW and NS components, respectively) are also shown for sites having earthquake data available.

Figure 12 - Light grey: sector of Benevento with no-significant site effects characterized by a nearly outcropping bedrock (seismic response of type I). Intermediate grey: sector characterized by mainly 1D high-frequency ($f \geq 4$ Hz) resonance of shallow layers overlaying the conglomeratic bedrock (type II). Dark grey: zones characterized by moderate broad-band (1-10 Hz) amplifications related to a thick layering of soft-to-consolidated fine soils overlaying stiff Pliocene terrains (type III). For each type of seismic response, the average of amplification factor (as defined in Eq. 4) and the 1 standard deviation are reported in the inset. The old town is bounded by a dashed black line.

TABLE 1. For each geological class, we indicate the range of shear-wave velocities (Vs) and a weighted value (<Vs>) used in 1D numerical modelling. Density values of continental deposits and Middle Pliocene clays are those reported by Marcellini et al. (1991) and Improta (1998) based on standard laboratory tests. The density assigned to the Middle Pliocene sandstones/conglomerates and to the Miocene melange has been proposed by Improta et al. (2003) based on gravity data modelling performed in the Sannio region.

CLASS	LITHOLOGY	ρ(t/mc)	Vs (m/s)	<Vs>
Near-surface Soils: Filling (F), Colluvial soils (Cl) and Slope Debris (Db)	Very soft fine soils with organic content, weathered pyroclastites (Cl) and debris of masonry (F). Loose sandy gravels and very soft silty clays (Db).	*1.7-1.8*	*200÷330*	*270*
Late Pleistocene-Holocene Alluvia ($Al_{2A,B}$)	Loose to dense sandy gravels and silty sands.	*1.8-2.0*	*330÷430*	*380*
Lower-Middle Pleistocene fluvio-lacustrine soils (Al_1) and Fine Ancient Alluvia (palustrine facies C - AA_C)	Soft to consolidated silty clays, with sandy lenses and peats.	*1.9* *2.0*	*shallow 320÷440* *deep 430÷610*	*360* *520*
Coarse Ancient Alluvia (facies B - AA_B)	Dense to very dense sandy gravels and silty sands.	*2.2*	*shallow 460÷600* *deep 860÷1210*	*530* *1090*
Coarse Ancient Alluvia (facies A - AA_A)	Stiff Cemented conglomerates.	*2.3*	*1000÷1730*	*1410*
Weathered Conglomerates (AA_{AW})	Very dense gravels.	*2.2*	-	*810*
Pliocene Clays (P_{ag})	Stiff silty clays.	*2.1*	*600÷800*	*710*
Superficial weathered Pliocene Clays (P_{agW})		*1.9*	*330÷540*	*350*
Pliocene Sandstones (P_s) Miocene Melange (M)	Sandstones with conglomerates. Shales, sandstones, marly limenstones.	*2.35*		*1300*

TABLE 2. Soil class as defined by EC8. V_{s30} is the average shear velocity in the uppermost 30 meters, computed as $V_{s30} = 30/(\Sigma_i h_i/v_i)$; N_{spt} are the numbers of hits for standard penetration test and c_u is the undrained cohesion. This classification is the one adopted by the national code (''Norme Tecniche per le Costruzioni'' of September 23, 2005).

Class	**Soil Description**	**Physical parameters**
A	Rock or other rock-like geological formation, including at most 5 m of weaker material at the surface	V_{s30} >800 m/s
B	Deposits of very dense sand, gravel, or very stiff clay, at least several tens of m in thickness, characterized by a gradual increase of mechanical properties with depth	360<V_{s30}<800 m/s N_{spt} >50 c_u >250 KPa
C	Deep deposits of dense or medium-dense sand, gravel or stiff clay with thickness from several tens to many hundreds of m	180< V_{s30} <360 15< N_{spt} <50 70< c_u <250 KPa
D	Deposits of loose-to-medium cohesionless soil(with or without some soft cohesive layers), or of predominantly soft-to-firm cohesive soil	V_{s30}< 180 m/s N_{spt}< 15 c_u<70 KPa
E	A soil profile consisting of a surface alluvium layer with average shear wave velocity* values of class C and D and thickness varying between about 5m and 20 m, underlain by stiffer material with V_{s30}>800 m/s	

*In the definition of Type E soil we follow the indication of ETC-12 Evaluation Committee for the Application of EC8 (Athens workshop, January 20-21, 2006).

TABLE 3. Amplification factor (AF) as defined by Eq. 4. For each site we also indicate the soil class. The last column shows the typology of seismic response as discussed in the text.

Site	Soil Class	Amplification Factors			Type of Seismic Response
		Molise (*EGF*)	Irpinia (*EGF*)	Irpinia (*input Sturno*)	
ARC1	A	1	1	1	I
MUS1	A		1.2	1.0	I
CAL1	E			1.5	II
CAL3	E			1.4	II
CAL4	B	1.5		1.8	II
CRE2	E		1.3		II
TEA1	C	1.5		2.0	III
SAB1	C		2.7		III
SAB4	B		2.0		III
SAB5	C	1.5	2.9		III

References

Aki, K. (1967). The scaling law of seismic spectrum, *J. Geophys. Res.* **72**, 1217-1231.

Bard, P.Y. (1999). Microtremor measurements: a tool for site effect estimation?, *State-of-the-art paper, Second International Symposium on the Effects of Surface Geology on seismic motion*, Yokohama, December 1-3, 1998, Irikura, Kudo, Okada and Sasatani Eds., Balkema, 3, 1251-1279.

Bardet, J.P., K. Ichii, and C.H. Lin (2000). EERA, A Computer Program for Equivalent-linear Earthquake site Response Analyses of Layered Soil Deposits, University of Southern California, Department of Civil Engineering .

Bernard, P., and A. Zollo (1989). The Irpinia (Italy) 1980 earthquake: Detailed analysis of a complex normal faulting, *J. Geophys. Res.* **94**, 1631-1647.

Bisio, L., R. Di Giovambattista, G. Milano, and C. Chiarabba (2004). 3-D earthquake locations and upper crustal structure of the Sannio-Matese region (southern Italy), *Tectonophysics* **385**, 121-136.

Bonnefoy-Claudet, S. (2004). Nature du bruit de fond sismique: Implications pour les études des effets de site. *Ph.D. thesis*,University Joseph Fourier, Grenoble, France. (In French with English abstract).

Bonnefoy-Claudet, S., C. Cornou, P.Y. Bard, and F. Cotton (2006). H/V ratio: a tool for site effects evaluation. Results from 1D noise simulations. *Geophys. J. Int.* **167**, 827-837, doi:10.1111/j.1365-246X.2006.03154.x

Bonnefoy-Claudet, S., A. Koehler, C. Cornou, M. Wathelet, and P.Y. Bard (2007). Effects of Love waves on microtremors H/V ratio, *Bull. Seism. Soc. Am.*, in press

Borcherdt, R.D. (1970). Effect of local geology near San Francisco Bay, *Bull. Seism. Soc. Am.* **60**, 29-61.

Boschi, E., E. Guidoboni, G. Ferrari, D. Mariotti, G. Valensise, and P. Gasperini (2000). Catalogue of strong Italian earthquakes, *Annali di Geofisica* **43**, 4, pp. 268 (full database on CD-ROM).

Brune, J.N. (1970). Tectonic stress and the spectra of seismic shear waves from earthquakes, *J. Geophys. Res.* **75**, 4997-5009 (and correction, *J. Geophys. Res.* **76**, 5002).

Calderoni, G., A. Rovelli, G. Cultrera, R.M. Azzara, and G. Di Giulio (2005). Assessment of Ground Motions in Palermo (Italy) during the September 6, 2002, Mw 5.9 , *Bull. Seism. Soc. Am.* **95**, 6, 2342-2363, doi:10.1785/0120050063, 2005.

Calderoni, G., A. Rovelli, G. Milana, and G. Valensise (2007). Low stress drop in the October-November 2002 earthquakes in Molise, central-southern Italy: evidence for reutilization of Mesozoic faults?, *J. Geophys. Res*, submitted 2007.

Cara, F., G. Cultrera, R.M. Azzara, V. De Rubeis, G. Di Giulio, M.S. Giammarinaro, P. Tosi, P. Vallone, and A. Rovelli (2007). Microtremor Measurements in the City of Palermo, Italy: Analysis of the Correlation with Local Geology and Damage, *Bull. Seism. Soc. Am.* , submitted 2007.

Castenetto, R., and R. Romeo (1992). Il terremoto del Sannio del 5 Giugno 1688: analisi del danneggiamento subito dalla città di Benevento, *Atti 11° Convegno G.N.G.T.S.*, Roma, 1992.

CEN (Comité Européen de Normalisation), (2003). Eurocode 8: *Design of Structures for Earthquake Resistance. Part 1: General rules, seismic actions and rules for buildings.* stage 49 draft, Brussels.

Chiarabba, C., and A. Amato (1997). Upper crustal structure of the Benevento area (Southern Italy): Fault heterogeneities and potential for large earthquakes, *Geophys. J. Int.* **130**, 229-239.

912 Cocco, M., and A. Rovelli (1989). Evidence for the variation of stress drop between normal and thrust
913 faulting earthquakes in Italy, *J. Geophys. Res.* **94**, 9399-9416.
914
915 Cosenza, E., G. Manfredi, M. Polese, and G.M. Verderame (2005). Una metodologia per l'analisi della
916 vulnerabilità sismica di classi di edifici in c.a.: l'applicazione al Rione Libertà di Benevento, *Convegno*
917 *GNDT*, *Ext. Abst.*, Genova 15-16 February 2005.
918
919 D'Onofrio, A., F. Santucci de Magistris, and F. Vinale (2005). Caratterizzazione geotecnica ed analisi della
920 vulnerabilità sismica del sottosuolo per il comune di Benevento, *Convegno GNDT*, *Ext. Abst.,* Genova 15-16
921 February 2005.
922
923 Duval A.M., 1994. Détermination de la réponse d'un site aux séismes à l'aide du bruit de fond: évaluation
924 expérimentale. *Université Pierre-et-Marie Curie, Ph.D. Thesis (In french)*, 264pp., Paris, France
925
926 ETC-12. Geotechnical evaluation and application of the seismic Eurocode EC8 2003-2006 (2006).
927 *Proceedings of the Athens Workshop*, January 20 & 21 2006, Edited by G. Bouckovalas
928
929 Fäh, D., and P. Suhadolc (1994). Application of numerical wave-propagation techniques to study local soil
930 effects: the case of Benevento (Italy), *Pageoph*. **143**, 4, 513-536.
931
932 Field, E.H., and K.H. Jacob (1995). A comparison and test of various site-response estimation techniques,
933 including three that are not reference-site dependent, *Bull. Seism. Soc. Am.* **85**, 1127-1143.
934
935 Gueguen, P., C. Cornou, S. Garambois, and J. Banton (2007). On the Limitation of the H/V Spectral Ratio
936 Using Seismic Noise as an Exploration Tool: Application to the Grenoble Valley (France), a Small Apex
937 Ratio Basin, *Pure Appl. Geophys.* **164**, 115–134, doi 10.1007/s00024-006-0151-x.
938
939 Hartzell, S.H. (1978). Earthquake aftershocks as Green's Functions, *Geophys. Res. Lett.* **5**, 1-4.
940
941 Haskell, N.A. (1960). Crustal reflection of plane SH waves, *J. Geophys. Res*. **65**, 4147-4150.
942
943 Konno, K., and T. Ohmachi (1998). Ground motion characteristics estimated from spectral ratio between
944 horizontal and vertical components of microtremor, 1998, *Bull. Seism. Soc. Am.* **88**, 1, 228-241.
945
946 Iannaccone, G., L. Improta, G. Biella, M. Castellano, A. Deschamps, R. De Franco, L. Malagnini, L.
947 Mirabile, R. Romeo, and A. Zollo A. (1995). A study of local site effects in the Benevento town (Southern
948 Italy) by the analysis of seismic records of explosions, *Annali di Geofisica* **38**, n.3-4, 411-428.
949
950 Improta, L. (1998). Studio degli effetti delle eterogeneità geologiche a scala crostale e locale sulla
951 propagazione della radiazione sismica: applicazioni alla regione del Sannio, *University of Naples, Ph.D.*
952 *Thesis*, 184pp., Naples, Italy.
953
954 Improta, L., L. Bonagura, P. Capuano and G. Iannaccone (2003). An integrated geophysical investigation of
955 the upper crust of the epicentral area of the 1980, Ms 6.9, Irpinia earthquake (Southern Italy).
956 *Tectonophysics, 361 (1-2), 139-169*.
957
958 Improta, L., G. Di Giulio, and A. Rovelli (2005). Variations of local seismic response in Benevento
959 (Southern Italy) using earthquakes and ambient noise recordings, *J. Seism*. **9**, 191-210.
960
961 Joyner, W.B. and D.M. Boore (1986). On simulating large earthquakes by Green's function addition of
962 smaller earthquakes , in *Earthquake Source Mechanics*, Maurice Ewing Series 6, S. Das, J. Boatwright, and
963 C. Sholtz Eds., American Geophysical Monograph 37, Washington, D.C., 269-274.
964
965 Lanzo, G. (1996). Modulo di taglio iniziale di alcuni terreni naturali da prove di sito ed in laboratorio, in
966 *Studi e Ricerce del Dip. di Ingegneria Strutturare e Geotecnica*, Università La Sapienza, Roma, 21-96.
967
968 Lermo, J., and F.J. Chàvez-Garcia (1994). Are microtremors useful in site response evaluation?, *Bull. Seism.*

969 *Soc. Am.* **84**, 5, 1350-1364.
970
971 Marcellini A., P.Y. Bard, F. Vinale, J.C. Bousquet, D. Chetrit, A. Deschamps, L. Franceschina, B. Grellet, G.
972 Iannaccone, E. Lentini, T. Pescatore, F. Rippa, R. Romeo, M. Romito, B. Sauret, R. Scarpa, A. Simonelli, A.
973 Tento, and S. Vidal (1991). Benevento seismic risk project: Progress Report. *Proceedings of the Fourth*
974 *International Conference on Seismic Zonation*, Stanford, California, **I**, 605-669.
975
976 Marcellini, A., G. Iannaccone, R. Romeo, F. Silvestri, P.Y. Bard, L. Improta, J.P. Meneroud, P. Mouroux, C.
977 Mancuso, F. Rippa, A. Simonelli, P. Soddu, A. Tento, and F. Vinale (1995a). Benevento seismic risk project:
978 seismotectonic and geothecnical background. *Proceedings of the Fifth International Conference on Seismic*
979 *Zonation*, October 17-19, 1995, Nice, France, I, 802-809.
980
981 Marcellini, A., P.Y. Bard, G. Iannaccone, J.P. Meneroud, P. Mouroux, R. Romeo, F. Silvestri, A. Duval, C.
982 Martin, and A. Tento (1995b). The Benevento seismic risk project: The microzonation. *Proceedings of the*
983 *Fifth International Conference on Seismic Zonation*, October 17-19, 1995, Nice, France, I, 810-814.
984
985 Maresca, R., M. Castellano, R. De Matteis, G. Saccorotti, and P. Vaccariello (2003). Local site effects in the
986 town of Benevento (Italy) from noise measurements, *Pure Appl. Geophys.* **160**, 1745-1764,
987 doi:10.1007/s00024-003-2376-2.
988
989 Marrara, F. and P. Suhadolc (1998). Site amplifications in the city of Benevento (Italy): comparison of
990 observed and estimated ground motion from explosive sources, *J. Seism*. **2**, 125-143.
991
992 Mayer-Rosa, D. (1989). Critical parameter investigation for earthquake hazard calculation in the TERESA
993 test area of Sannio-Matese, *Natural Hazards **2***, 237-247.
994
995 Mayer-Rosa, D. (ed.) (1991). TERESA Project: earthquake hazard assessment in Sannio-Matese Southern
996 Italy, *Proc. Fourth International Conference on seismic zonation, Stanford, California, Vol. **I***, 591-603.
997
998 Nakamura, Y., (1989). A method for dynamic characteristics estimation of subsurface using microtremor on
999 the ground surface, *QR of RTRI* **30**, 25-33.
1000
1001 Ordaz, M., J. Arboleda, and S.K. Singh (1995). A scheme of random summation of an empirical Green's
1002 function to estimate ground motions for future large earthquakes, *Bull. Seism. Soc. Am.* **85**, 1635-1647.
1003
1004 Panou, A.A., N. Theodulidis, P. Hatzidimitriou, K. Stylianidis, and C.B. Papazachos (2005). Ambient noise
1005 horizontal-to-vertical spectral ratio in site effects estimation and correlation with seismic damage distribution
1006 in urban environment: the case of the city of Thessaloniki (Northern Greece), *Soil Dynamics and Earthquake*
1007 *Engineering* **25***,* 261–274.
1008
1009 Parolai, S. and S.M. Richwalski (2004). The importance of converted waves ib comparing H/V and RSM site
1010 response estimates, *Bull. Seism. Soc. Am.* **94**, 304-313.
1011
1012 Pecce, M., M. Polese, and G.M. Verderame (2004). Seismic vulnerability aspects of RC buildings in
1013 Benevento, in *The many facets of seismic risk*, CRdC-AMRA Edited by M. Pecce, G. Manfredi and A. Zollo,
1014 134-141.
1015
1016 Pescatore, T., L. Improta, R. Romeo, and G. Iannaccone (1996). Geologia della citta' di Benevento:
1017 caratteristiche litostratigrafiche finalizzate alla microzonazione sismica, *Boll. Soc. Geol. It.* **115**.
1018
1019 Pescatore, T., M.R. Senatore, and M. Boscaino (2005). La geologia di Benevento: un modello fisico del
1020 sottosuolo per lo studio della risposta sismica, *Convegno Nazionale GNGDT, Ext. Abst.,* Genova 15-16
1021 February 2005.
1022
1023 Sabetta, F. and A. Pugliese (1996). Estimation of response spectra and simulation of nonstationary
1024 earthquake ground motions, *Bull. Seism. Soc. Am.* **86**, 337-352.
1025

SESAME Project (2004). Site EffectS using AMbient Excitations, http://sesame-fp5.obs.ujf-grenoble.fr

Silvestri, F. (1991). Stress-strain behaviour of natural soils by means of cyclic/dynamic torsional shear test, *Proc. Symphosium on experimental characterization and modelling of soils and soft rocks*, Naples, Italy.

Traiano Project (2002). Project for the assessment and the reduction of vulnerability of urban areas, http://www.ingv.it/gndt/Att_scient/PE2002_Brief_Reports/brief_reports_con_int.htm

Tucker, B., and J. King (1984). Dependence of sediment-filled valley response on input amplitude and valley properties, *Bull. Seism. Soc. Am.* **74**, 153-165.

Valensise, G., D. Pantosti, and R. Basili (2004). Seismology and tectonic setting of the Molise earthquake sequence of October 31 – November 1 2002, *Earthquake Spectra* **20**, 1-15.

Wennerberg, L. (1990). Stochastic summation of empirical Green's functions, *Bull. Seism. Soc. Am.* **80**, 1418-1432.

Westaway, R. (1987). The Campania, Southern Italy, earthquake of 1962 August 21, *Geophys. J. R. Astr. Soc.* **88**, 1-24.

Westaway, R., and J. Jackson (1987). The earthquake of the 1980 Novembre 23 in Campania Basilicata (Southern Italy), *Geophy. J. R. Astr. Soc.* **90**, 375-443.

Figure1

Click here to download high resolution image

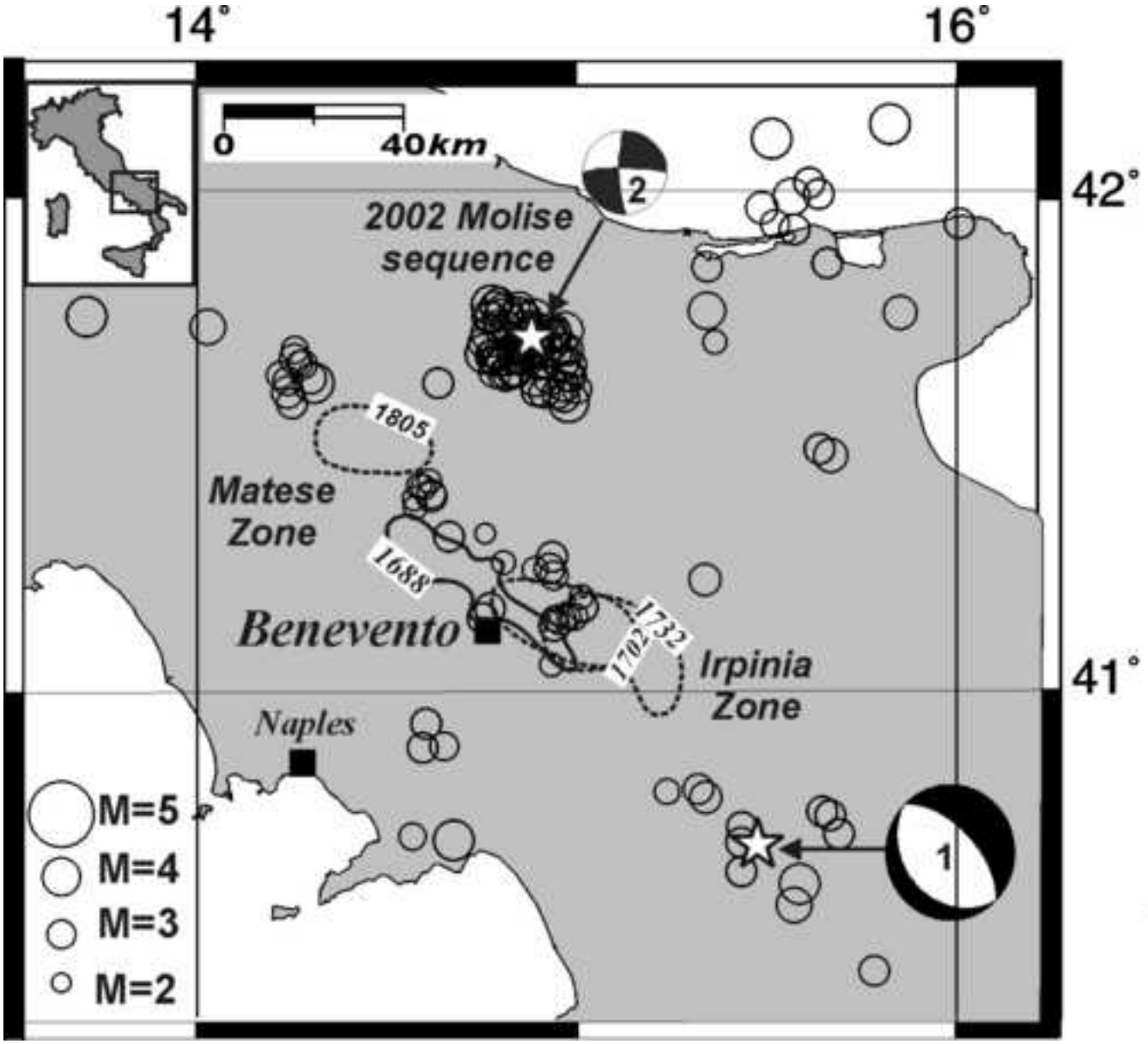

Figure2

Click here to download high resolution image

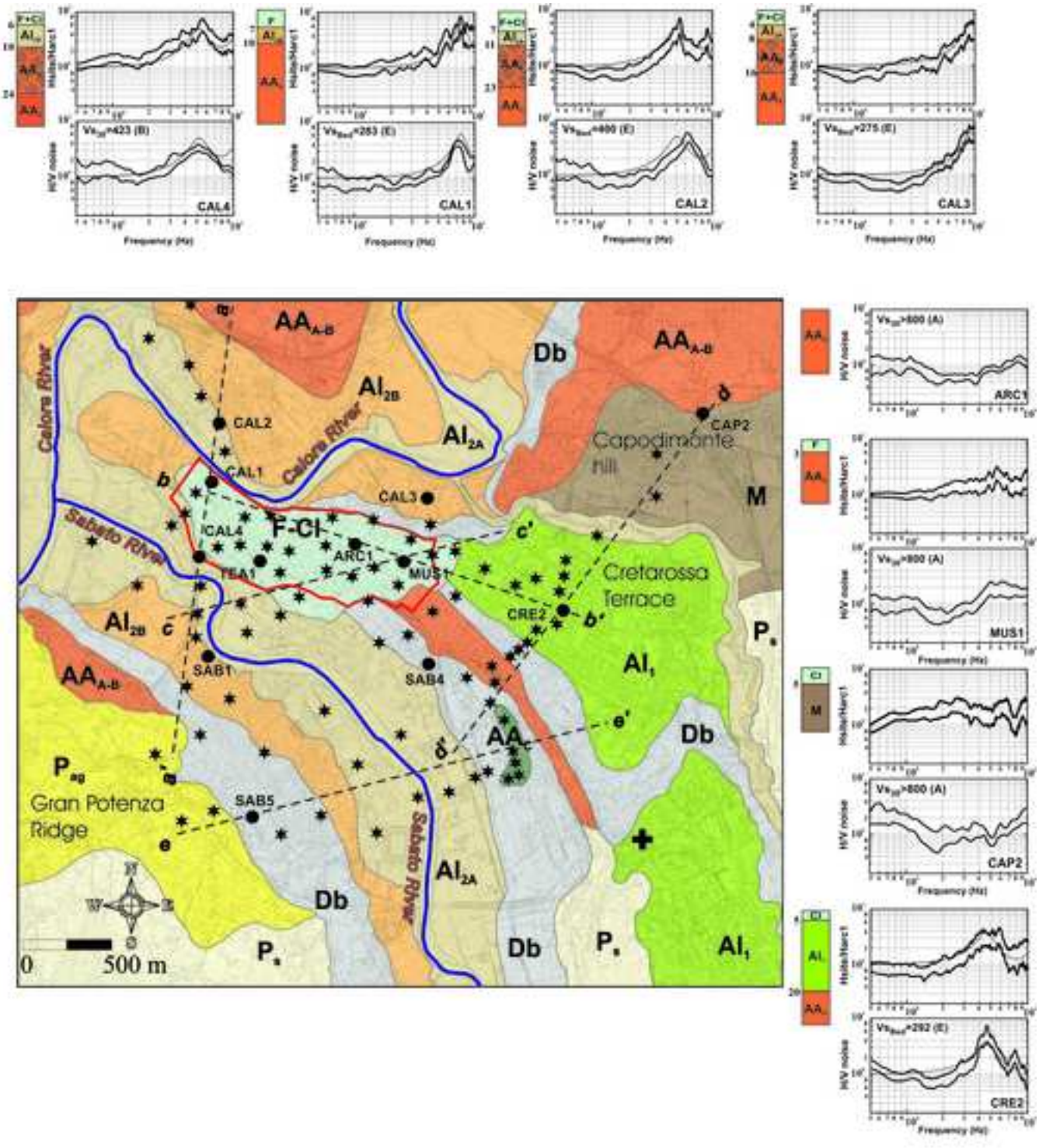

Figure3

Click here to download high resolution image

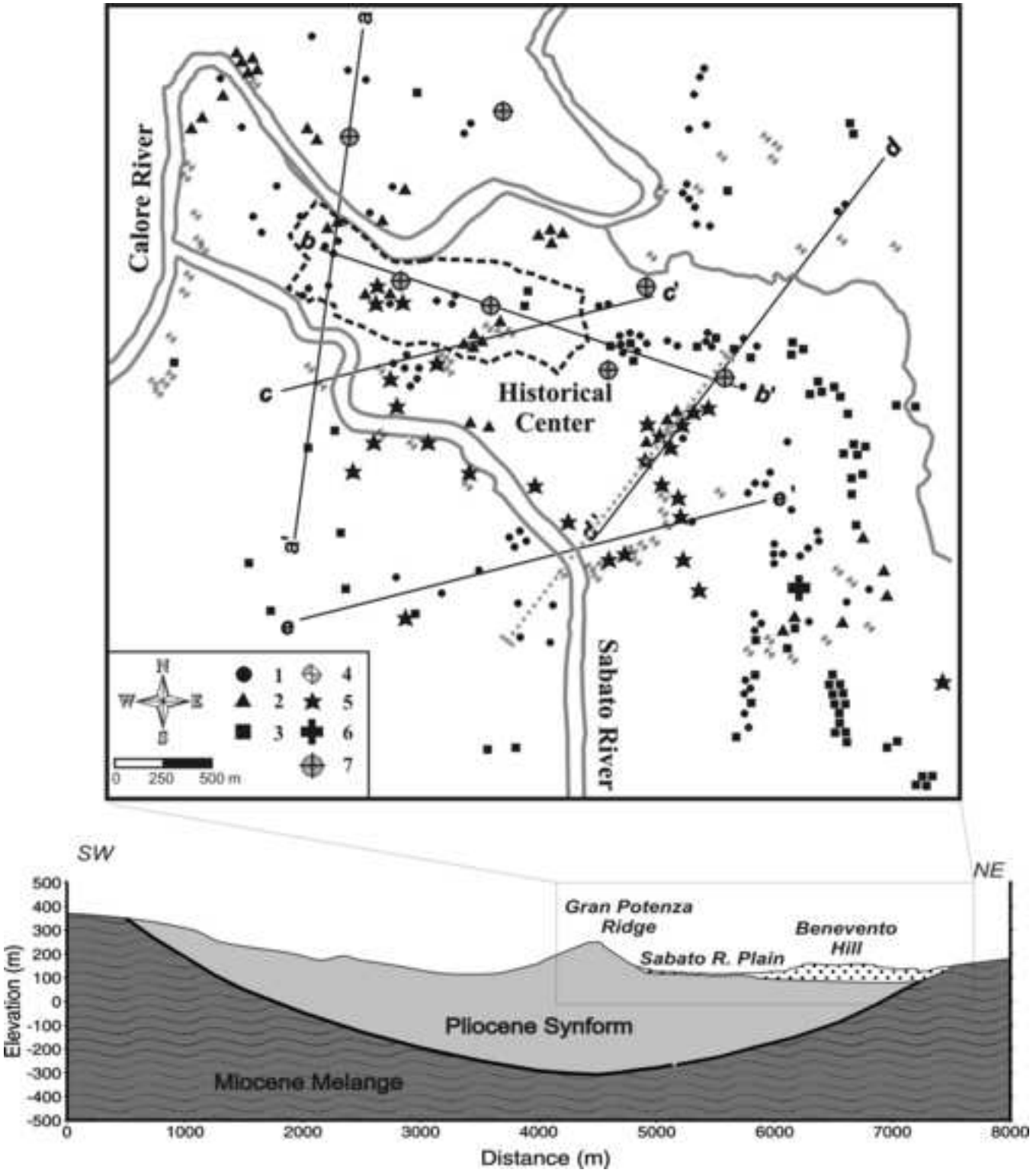

Figure4

Click here to download high resolution image

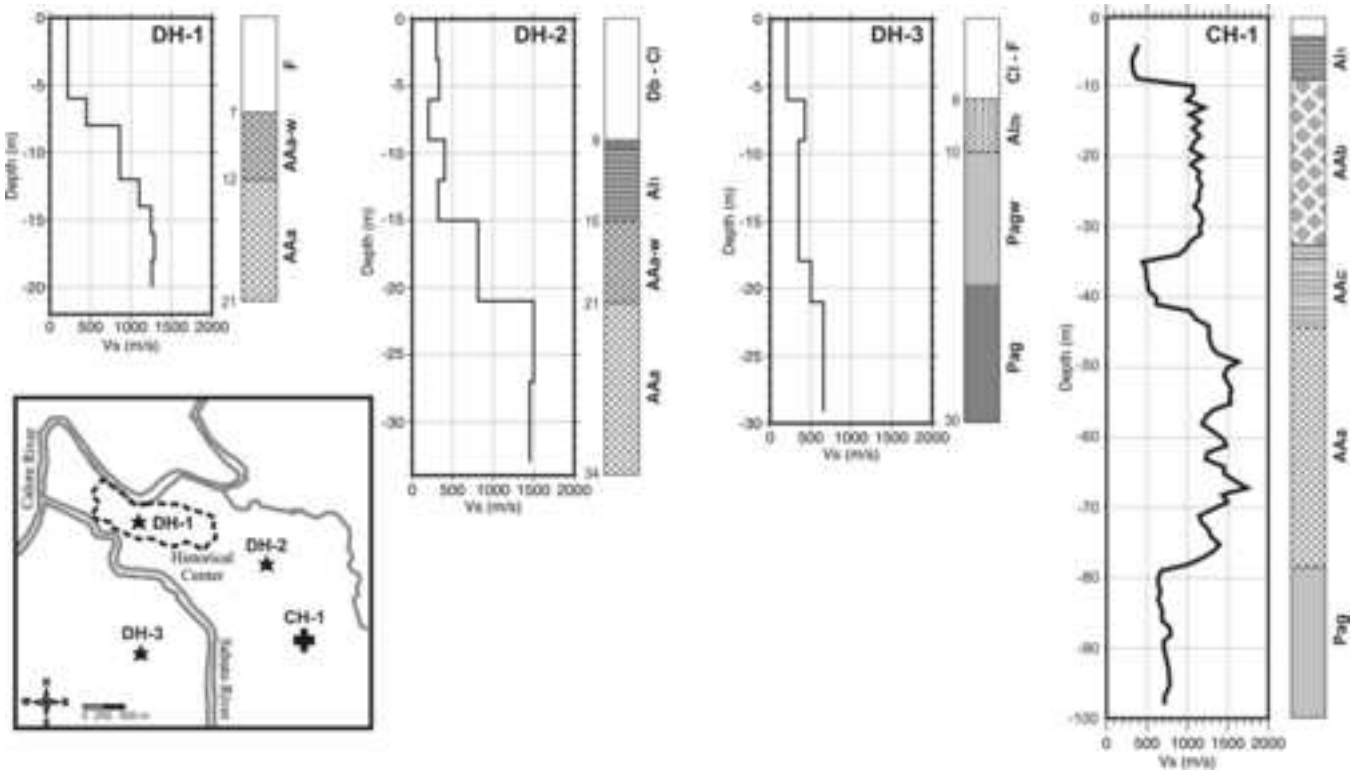

Figure5a

Click here to download high resolution image

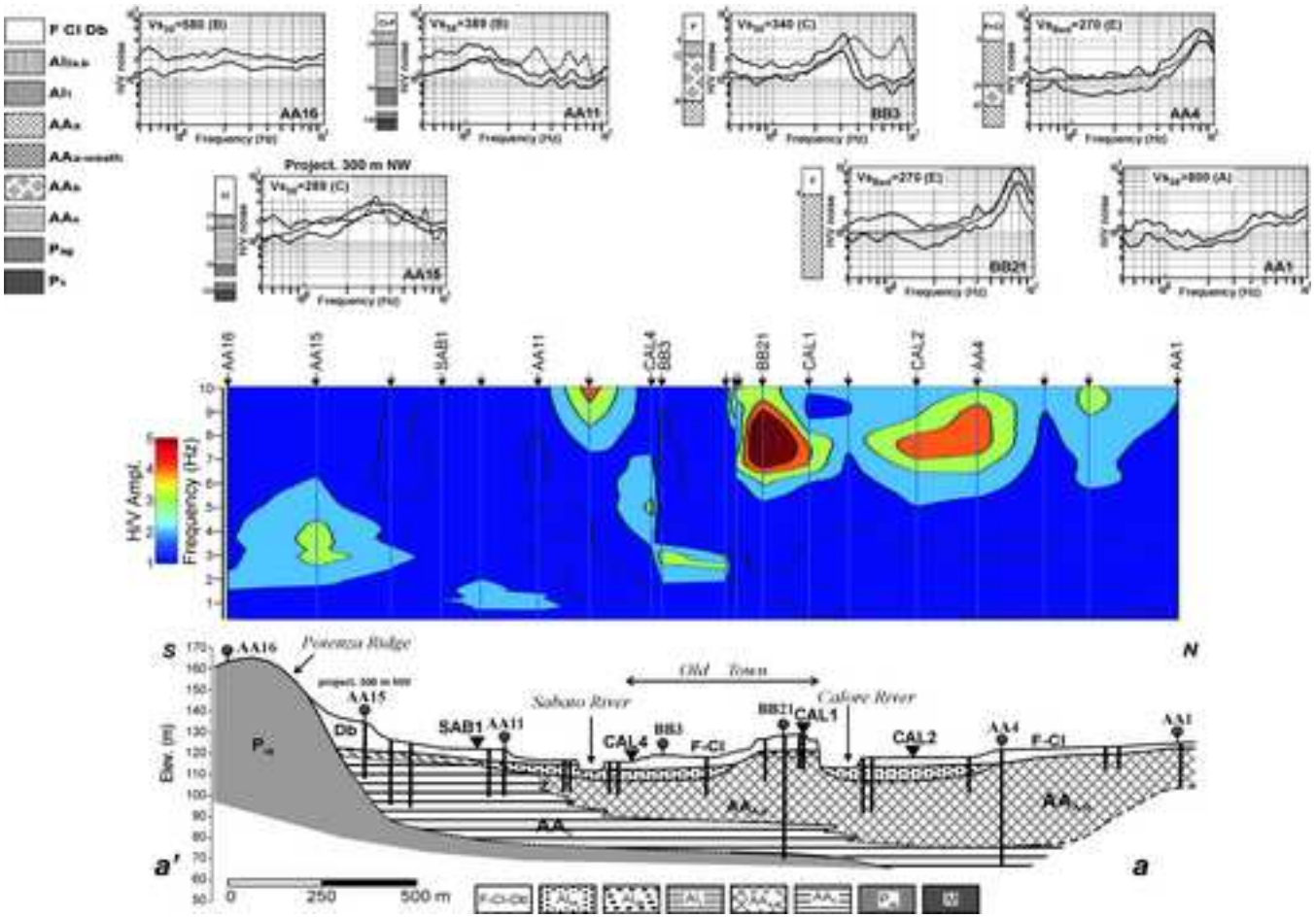

Figure5b

Click here to download high resolution image

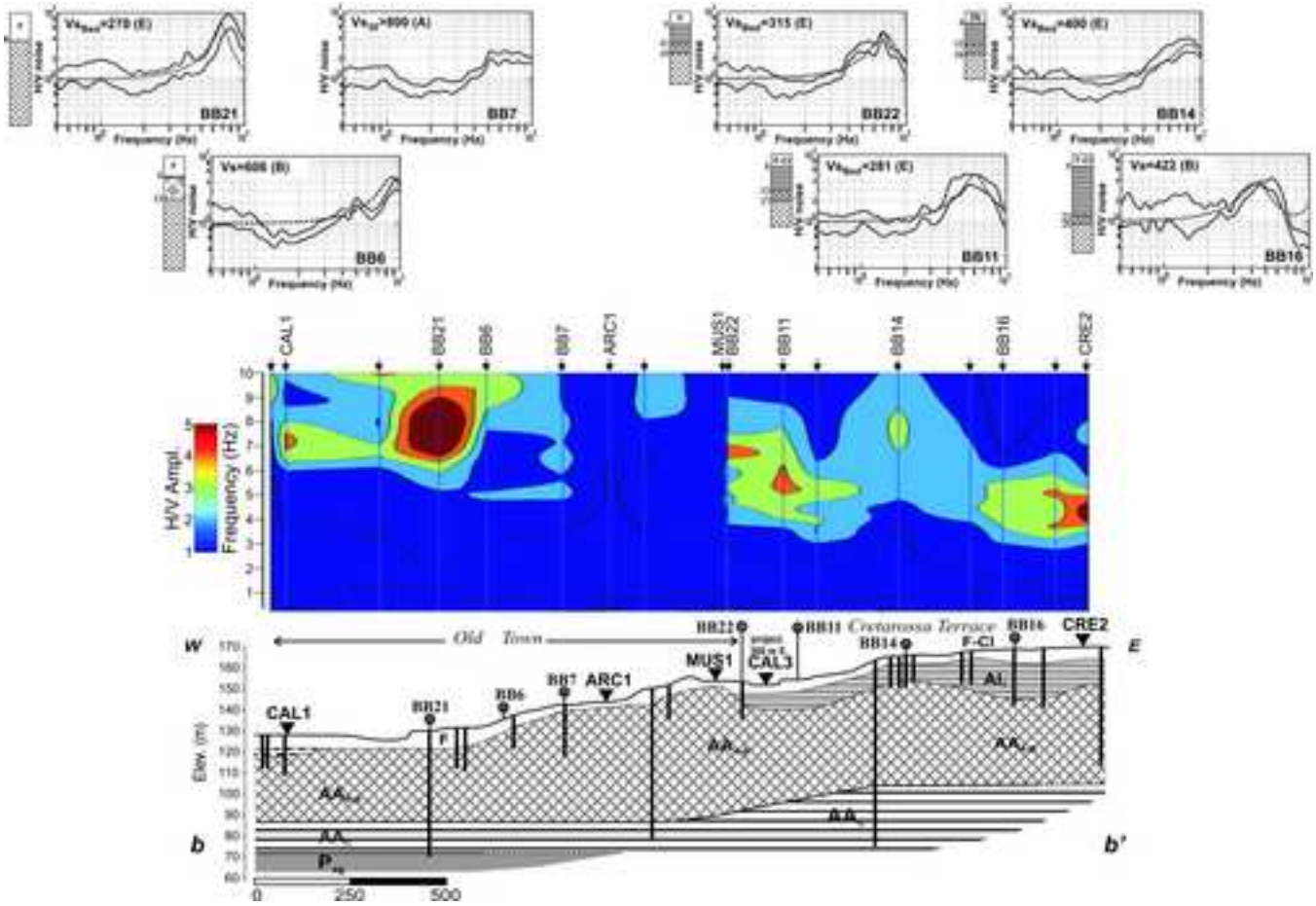

Figure5c

Click here to download high resolution image

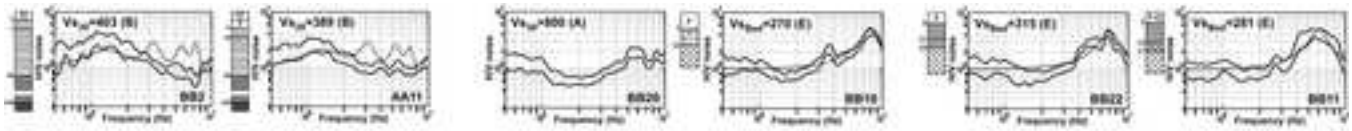

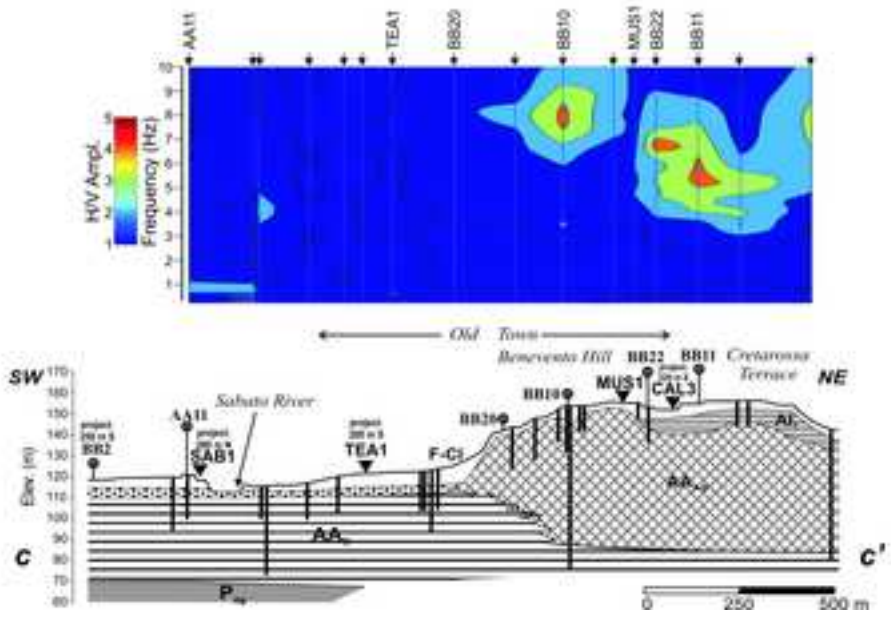

Figure5d

Click here to download high resolution image

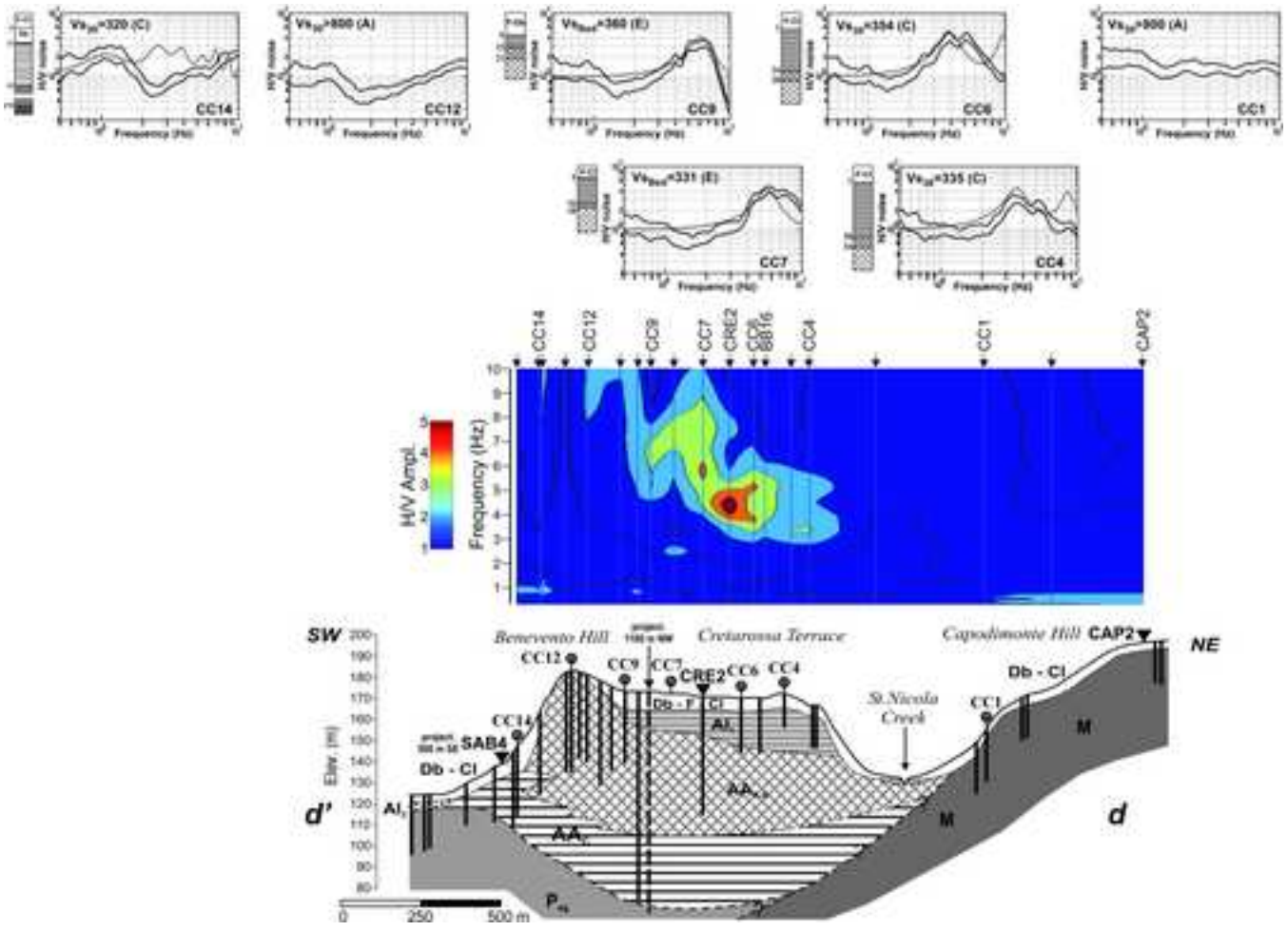

Figure5e

Click here to download high resolution image

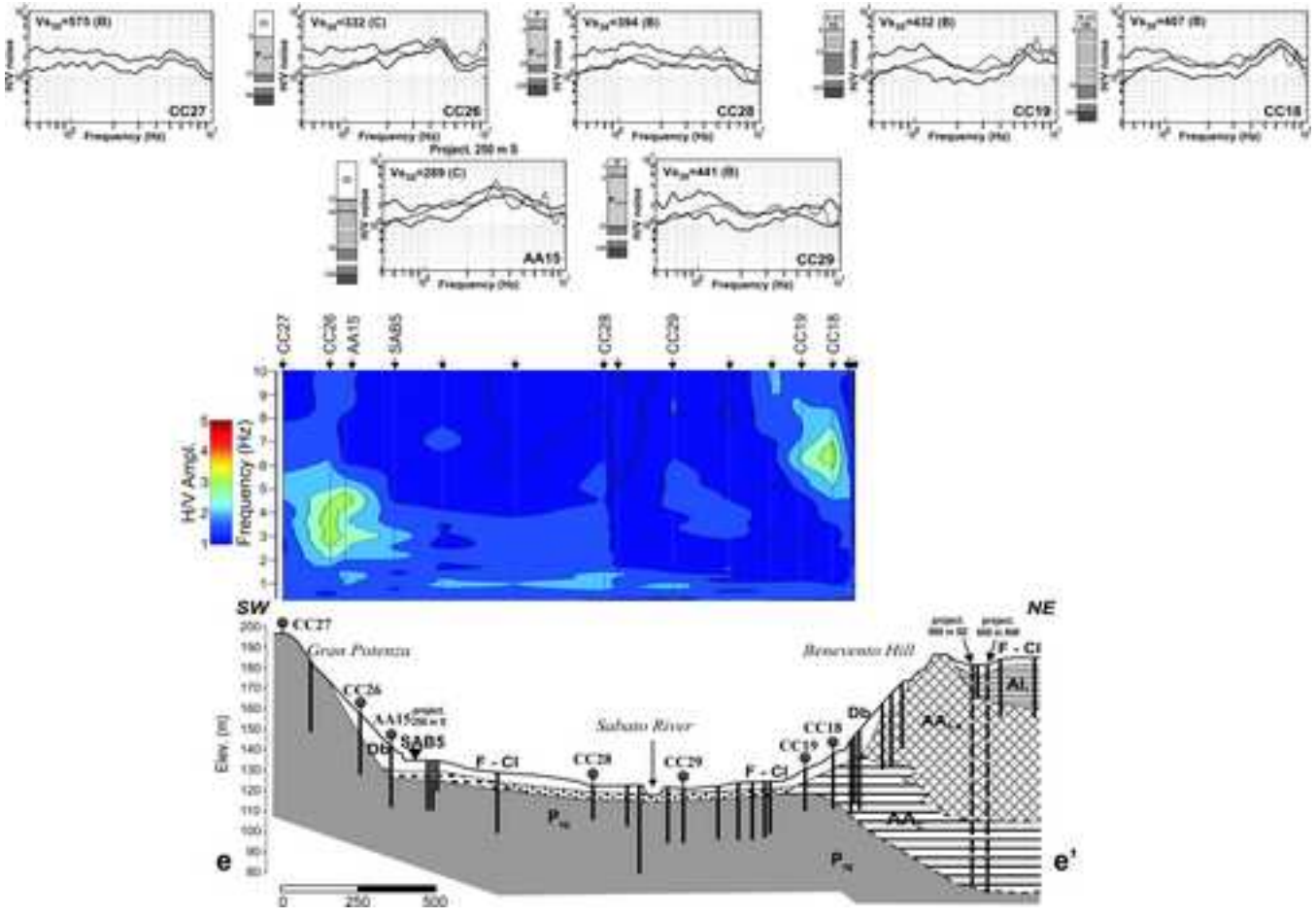

Figure5f

Click here to download high resolution image

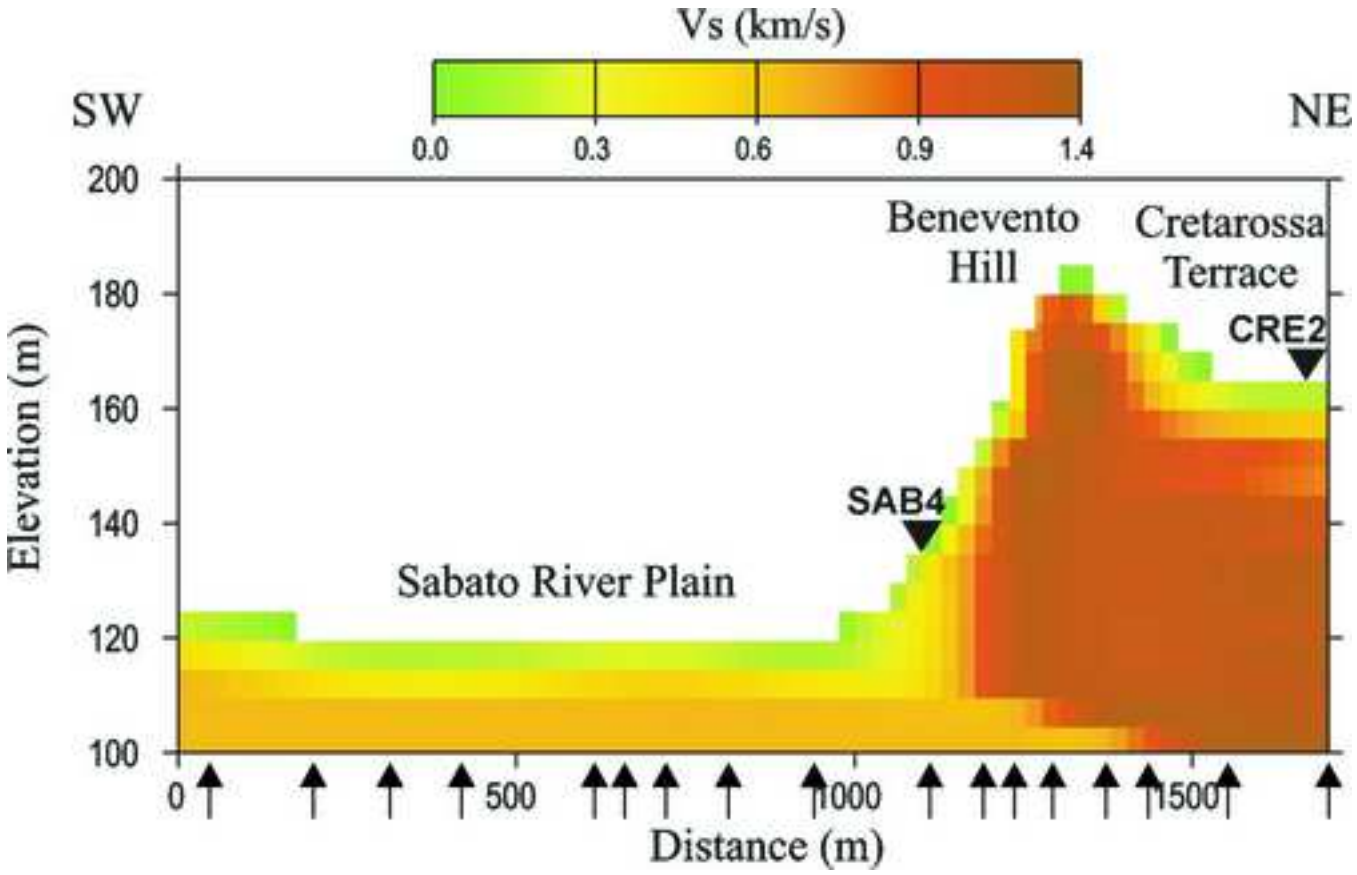

Figure6

Click here to download high resolution image

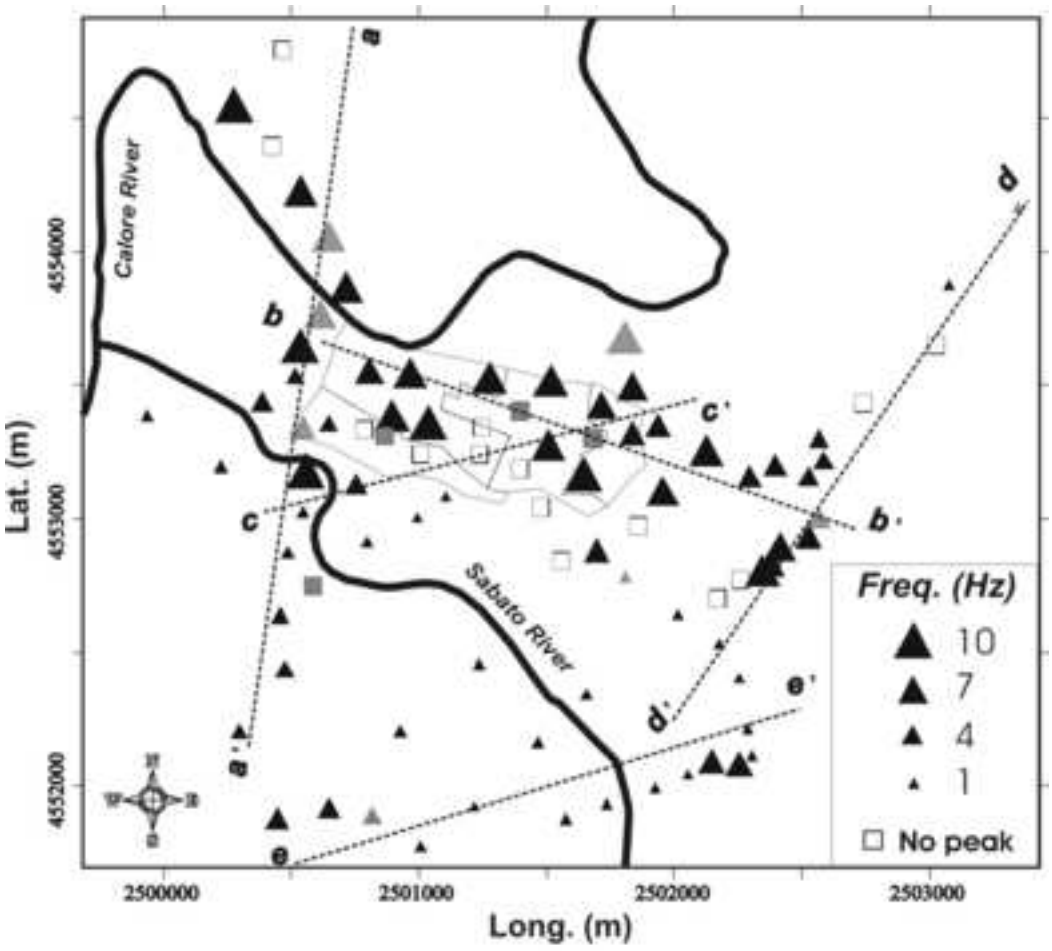

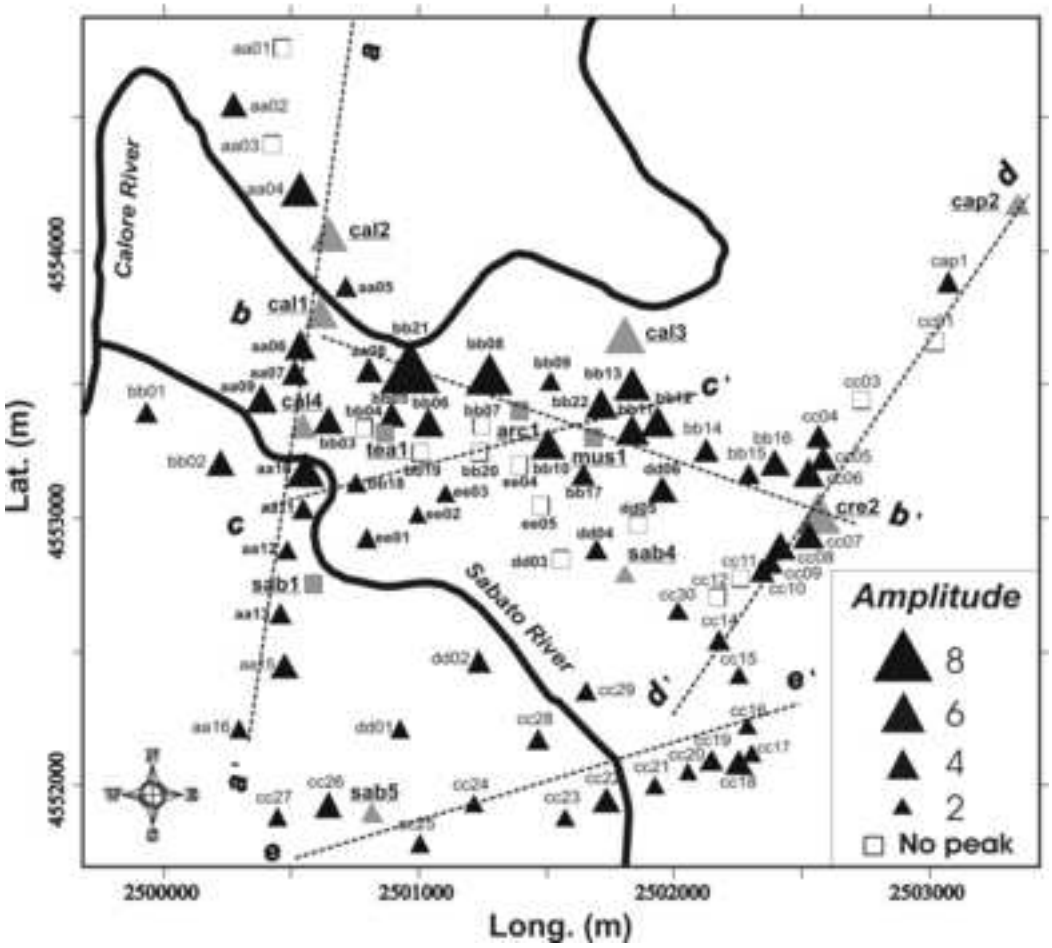

Figure7

Click here to download high resolution image

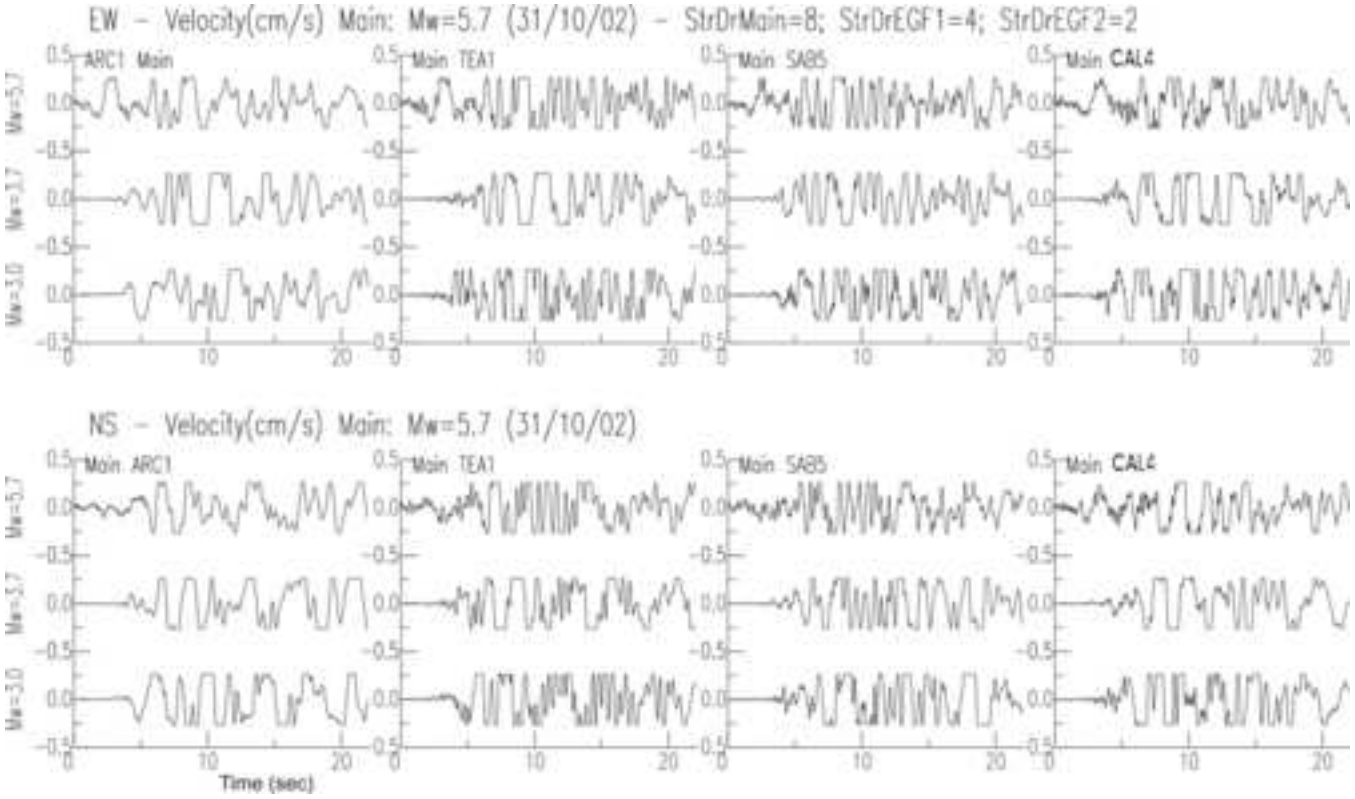

Figure8

Click here to download high resolution image

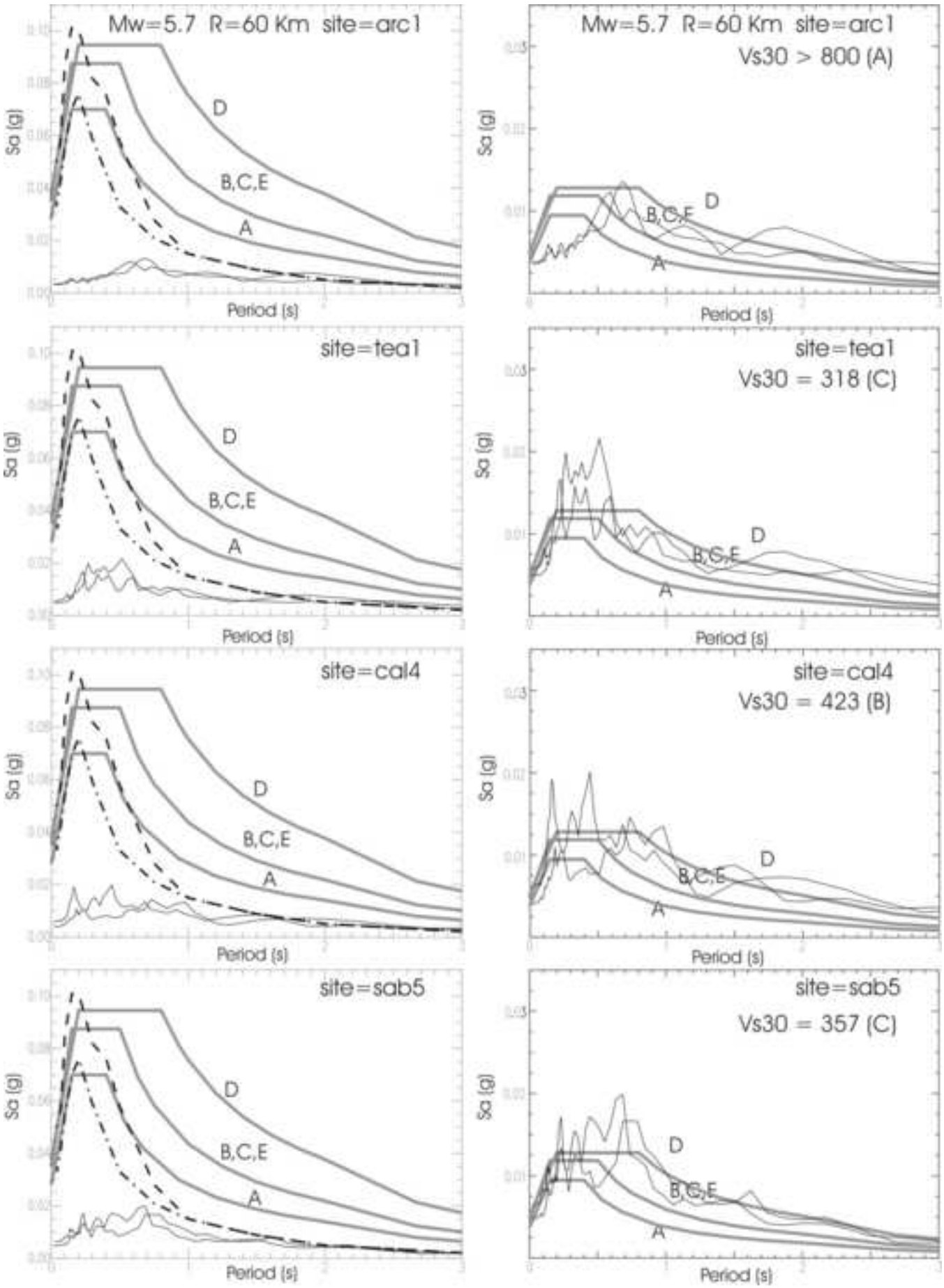

Figure9

Click here to download high resolution image

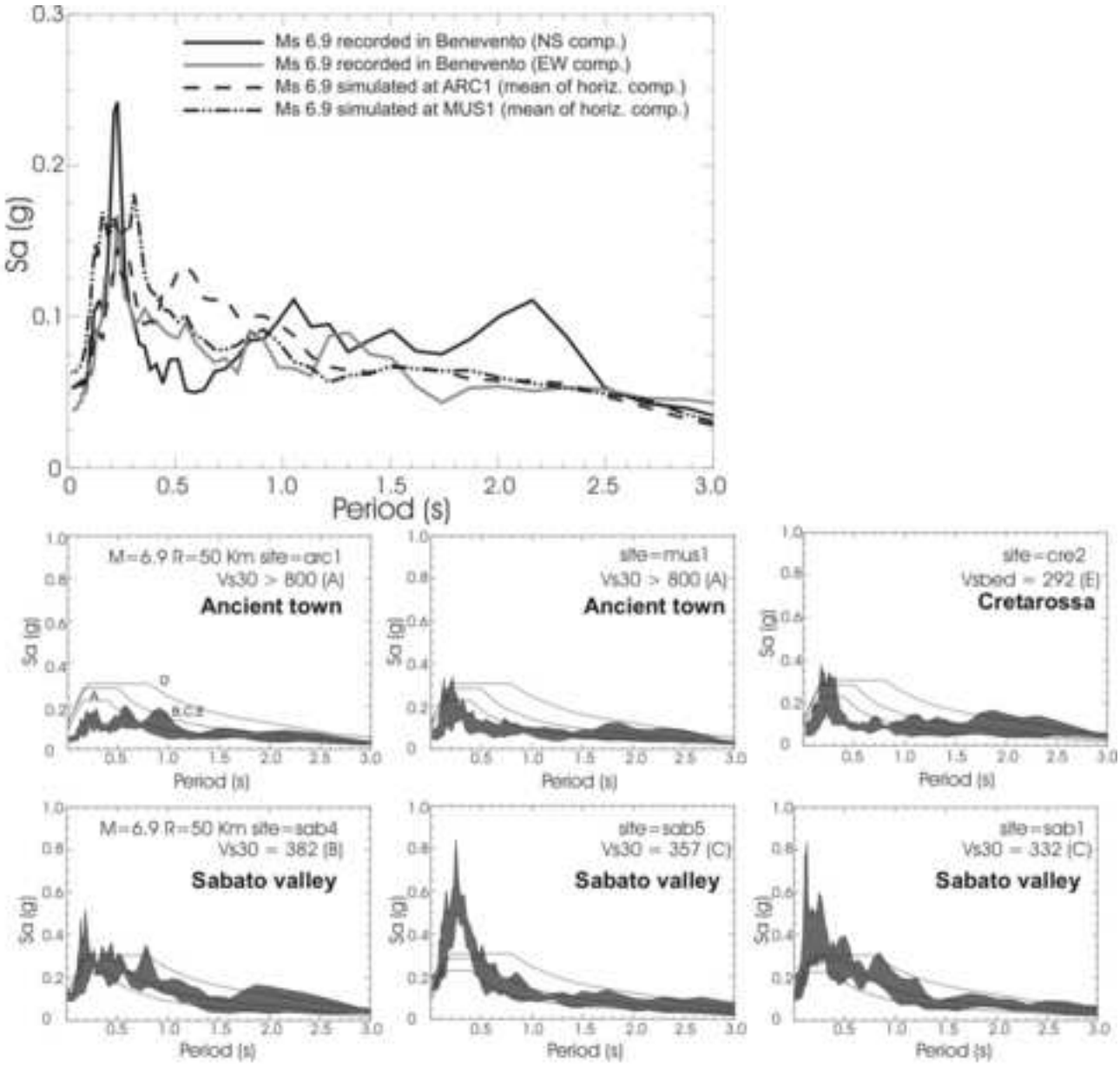

Figure10

Click here to download high resolution image

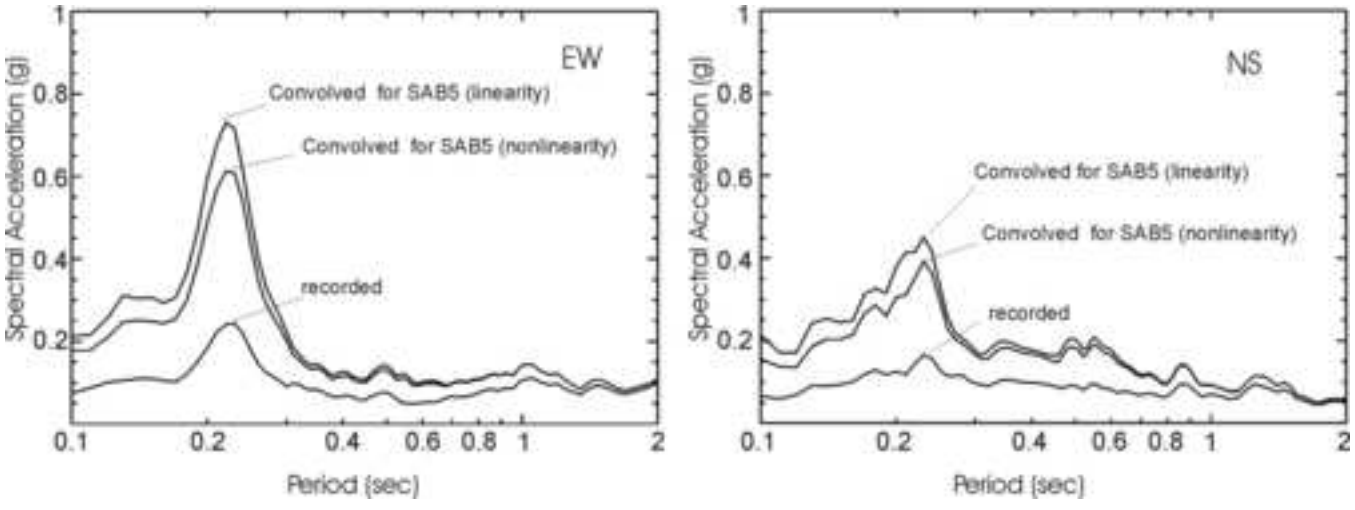

Figure11

Click here to download high resolution image

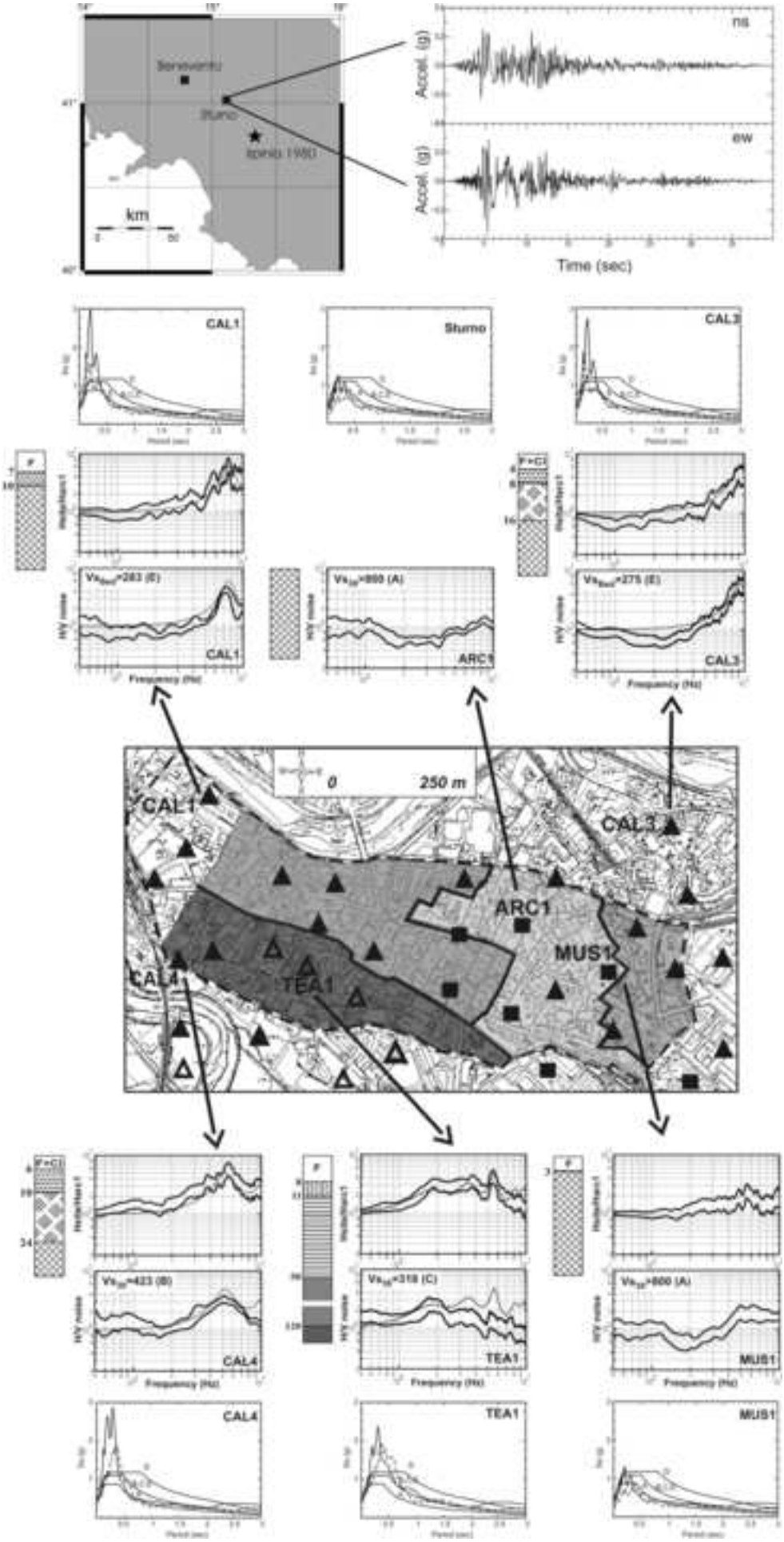

Figure12

Click here to download high resolution image